NASA CR 159864

A CALCULATION PROCEDURE FOR VISCOUS FLOW IN TURBOMACHINES - VOL. III

BY

I. KHALIL, Y. SHEORAN AND W. TABAKOFF

(NASA-CR-159864) A CALCULATION PROCEDURE FOR VISCOUS FLOW IN TURBOMACHINES, VOLUME 3 (Cincinnati Univ.) 46 p HC A03/MF A01 CSCL 01A N80-26274 Unclas G3/02 27863

Supported by:

U.S. Army Research and Technology Laboratories

(AVRAD COM)

Lewis Research Center

Contract No. NAS3-21609

JUNE 1980

NASA CR 159864

A CALCULATION PROCEDURE FOR VISCOUS FLOW IN TURBOMACHINES - VOL. III

by

I. Khalil, Y. Sheoran and W. Tabakoff

Supported by:

U.S. Army Research and Technology Laboratories

(AVRAD COM)

Lewis Research Center

Contract No. NAS3-21609

JUNE 1980

1. Report No.	2. Government Accession No.	3. Recipient's Catalog No.
NASA CR 159864		

4. Title and Subtitle	5. Report Date
A CALCULATION PROCEDURE FOR VISCOUS FLOW IN TURBOMACHINES - VOL. III	JUNE 1980
	6. Performing Organization Code
7. Author(s)	8. Performing Organization Report No.
I. KHALIL, Y. SHEORAN AND W. TABAKOFF	
9. Performing Organization Name and Address	10. Work Unit No.
DEPT. OF AEROSPACE ENGINEERING & APPLIED MECHANICS UNIVERSITY OF CINCINNATI CINCINNATI, OHIO 45221	11. Contract or Grant No. NAS3-21609
12. Sponsoring Agency Name and Address	13. Type of Report and Period Covered Contract Report
U.S. ARMY RESEARCH & TECHNOLOGY LABORATORIES (AVRAD COM) PROPULSION LABORATORY LEWIS RESEARCH CENTER, CLEVELAND, OHIO 44135	14. Sponsoring Agency Code 1L161102AH45

15. Supplementary Notes

Topical Report. Project Manager, Dr. E. R. McFarland, Fluid Mechanics and Acoustics Division, NASA Lewis Research Center, Cleveland, Ohio 44135.

16. Abstract

A method for analyzing the nonadiabatic viscous flow through turbomachine blade passages is presented. The field analysis is based upon the numerical integration of the full incompressible Navier-Stokes equations, together with the energy equation on the blade-to-blade surface. A Fortran IV computer program has been written based on this method. The numerical code used to solve the governing equations employs a nonorthogonal boundary fitted coordinate system. The flow may be axial, radial or mixed and there may be a change in stream channel thickness in the through-flow direction.

The program input consists of the configuration of the stream channel annulus S_1, the blade-to-blade stream channel weight flow, the inlet flow conditions, the outlet flow angle, and the rotational speed of the machine. The output includes the distribution of the stream function, the vorticity, the static pressures within the blade passages, and the variation of meridional and tangential velocity components from blade-to-blade and from the inlet of the machine to its exit are moreover generated. The program also has the capability to generate the temperature distribution within the blade passages in case the blade cooling is under consideration.

This report includes a complete description of the inputs required for two Fortran IV programs. The first program considers laminar flows and the second can handle turbulent flows. Numerical examples have been included to illustrate the use of the program, and to show the results that are obtained.

17. Key Words (Suggested by Author(s))	18. Distribution Statement
Turbine Aerodynamics Cascade Flow	Unclassified - unlimited STAR Category 02

19. Security Classif. (of this report)	20. Security Classif. (of this page)	21. No. of Pages	22. Price*
UNCLASSIFIED	UNCLASSIFIED	42	

* For sale by the National Technical Information Service, Springfield, Virginia 22161

NASA-C-168 (Rev. 10-75)

TABLE OF CONTENTS

LIST OF FIGURES

FORTRAN PROGRAM FOR CALCULATING VISCOUS FLOW ON A BLADE-TO-BLADE STREAM SURFACE OF A TURBOMACHINE

SUMMARY

A method for analyzing the nonadiabatic viscous flow through turbomachine blade passages is presented. The field analysis is based upon the numerical integration of the full incompressible Navier-Stokes equations, together with the energy equation on the blade-to-blade surface. A Fortran IV computer program has been written based on this method. The numerical code used to solve the governing equations employs a nonorthogonal boundary fitted coordinate system. The flow may be axial, radial or mixed and there may be a change in stream channel thickness in the through-flow direction.

The program input consists of the configuration of the stream channel annulus S_1, the blade-to-blade stream channel weight flow, the inlet flow conditions, and outlet flow angle, and the rotational speed of the machine. The output includes the distribution of the stream function, the vorticity, the static pressures within the blade passages, and the variation of meridional and tangential velocity components from blade-to-blade and from the inlet of the machine to its exit are moreover generated. The program also has the capability to generate the temperature distribution within the blade passages in case the blade cooling is under consideration.

This report includes a complete description of the inputs required for two Fortran IV programs. The first program considers laminar flows and the second can handle turbulent flows. Numerical examples have been included to illustrate the use of the program, and to show the results that are obtained.

INTRODUCTION

An attempt is made to demonstrate the feasibility of obtaining viscous flow details within turbomachine passages by appropriately combining several blade-to-blade viscous flow solutions. Each of these solutions is obtained through the numerical integration of the full incompressible Navier-Stokes equations over a predetermined stream surface that extends between the blades. The set of stream surfaces required for the analysis are themselves generated from the solution of the nonviscous version of the Navier-Stokes equations.

This report is presented in two parts. Part I includes a description of the input to the laminar viscous flow Fortran IV program and the interpretation of its output. A numerical example has been included to demonstrate the use of the program. The example includes flow in a radial inflow turbine.

Part II presents the procedures for computing turbulent viscous flow details within turbomachine passages. This part discusses the input and output, with a numerical example to demonstrate its use as a turbulent viscous flow analyzer.

The present report forms the final volume of a three volume report. This volume is organized as a user's manual to serve an individual desiring to use the program. For those who wish to study the calculation procedures and the mathematical analysis in detail and need to modify the program to suit their needs, this report will have to be used in conjunction with the theoretical procedure which forms the contents of Vol. I and Vol. II [2, 7]. The entire report is organized such that a design engineer desiring the use the program need only read the sections NUMERICAL EXAMPLE and DESCRIPTION OF INPUT AND OUTPUT, of Part I alone or both Part I and Part II. If only laminar viscous flow details are needed then reading Part I would suffice. However, if turbulent viscous flow details are sought then both Part I and Part II should be read. Both sections have been organized into decimally numbered subsections, and accordingly a decimally numbered system is used for the equations and figures. This numbering system is adopted for the ease of handling the two parts with overlapping information and frequent cross references. In this decimal numbering system, the first number refers to the part of the report in which the section, equation or figure exists and the subsequent numbers refer to subsection.

PART I

1.1 NUMERICAL EXAMPLES

To illustrate the use of the program and to show the type of results which can be obtained, a numerical example is given.

Radial Inflow Turbine

An example turbine rotor profile is shown in Fig. 1.1. First a meridional plane analysis was made by the quasi-orthogonal method of reference [1] to establish the stream channel geometry and the stream annulus thickness distribution. The flow patterns are investigated on this blade-to-blade stream channel, S_1, located midway in the passage depth of the rotor as shown in Fig. 1.1. The results presented here are case 2 of reference [2]. The primary reason for the selection of this specific rotor is that a substantial amount of experimental data is available for comparison [3]. The input data for the program are given in Table 1.I. A sample of the output of the program is presented in Tabale 1.II. The streamlines are designated by the stream function ratio ψ/ψ_{total}. Such streamline contours are plotted in Fig. 1.2 along with the streamlines determined experimentally. Also presented here are the velocity profile at three radial locations as shown in Fig. 1.3. For the purpose of comparison the inviscid flow profiles, indicated by dotted lines, are superimposed on the viscous profiles in Fig. 1.3. For a more detailed discussion of these results, Vol. I of this report should be referred [2].

Radial Compressor Rotor

This example is a rotor of a radial bladed compressor of reference [4]. The rotor profile is shown in Fig. 1.4. First, a mid-channel stream surface, S_1, and the stream annulus thickness are calculated by the meridional flow analysis of reference [1]. A typical distribution of the flow properties on the blade-to-blade stream annulus, S_1, of Fig. 1.4 are calculated and the corresponding results are presented.

The results of radial compressor rotor flow are presented solely for the sake of demonstrating the capability of the program. Therefore only the final results are discussed. The preparation of input and interpretation of output is similar to the previous turbine example. A comparison between the predicted streamline contours and those determined experimentally in reference [4] are plotted in Fig. 1.5. The experimental evidence was obtained by tracing photographs of streak lines from the rotor segments under the same operating conditions reported here. A good agreement is generally observed. The predicted meridional velocity profiles across the rotor passage at three different radial locations are illustrated in Fig. 1.6. Shown also in the same figure, are the calculated velocity distribution using the inviscid blade-to-blade analysis of reference [5].

1.2 DESCRIPTION OF INPUT AND OUTPUT FOR LAMINAR VISCOUS FLOW PROGRAM

The computer program requires as input appropriate gas constants, operating conditions such as inlet temperature and density, inlet and outlet flow angles, weight flow, rotational speed, and information regarding the overlaying of grid in the flow passage. Figure 1.7 shows the m-θ coordinate system for a typical blade-to-blade surface which includes the physical flow domain. Also required as input is the stream surface geometry and transformation parameters at every grid point. The latter part of the input is obtained as a consequence of applying Thompson transformation to the blade. Output obtained from the program includes velocity magnitud and direction at all mesh points (meridional and tangential velocity), value of nondimensional vorticity, Reynolds number and pressure coefficients at each mesh point.

Input

Figure 1.8 shows the input form indicating the variables as they are punched on the data cards. There are two types of variables, geometric and nongeometric. The geometric input variables are shown in Figs. 1.9 and 1.10. A description of all the input variables is listed in this section.

Further explanation of key variables is given in the section, Instructions for Preparing Input. The input variables, in order of their appearance, are as follows:

AMU	Kinematic viscosity (N-s/m^2)
PRDNO	Prandtl number
TIP	Total inlet temperature of the turbine (°K)
TBLADE	Blade temperature (°K)
RHOIP	Total inlet density (Kg/m^3)
WTFL	Mass flow rate per blade, per stream channel, (Kg/sec)
OMEGA	Rotational speed of the machine (revolutions/sec)
BTI	Inlet flow angle to the machine (deg), (see Fig. 1.9)
BTO	Outlet flow angle to the machine (deg),(see Fig. 1.9)
BLADE	Number of blades
BIN	Inlet stream channel thickness, (m)
RTIP	Tip radius of the rotor, (m)
RIN	Inlet radius of the machine at upstream boundary AN, (m)
MXBI	Number of vertical mesh lines from AN to BM inclusive, (fig. 1.10)
MXBO	Number of vertical mesh lines from AN to FI inclusive, (Fig. 1.10)
MX	Total number of vertical mesh lines in m-direction from AN to GH; maximum of 50, (Fig. 1.10)
NBBI	Number of mesh spaces on ϕ direction between AB and NM; maximum of 30 (Fig. 1.10)
ITRB	-1 for turbine case; +1 for compressor
IPRINT	The number of iterations after which the output should be printed.

ISPL	For a straight blade, ISPL is assigned any integer value other than zero, otherwise it is left blank or zero. If ISPL is zero, then appropriate number of transformation parameters follow the stream surface configuration
AMM(I)	Array of m coordinate corresponding to mesh points (m)
R(I)	Array of r coordinate corresponding to AMM(I) array, (m)
SAL(I)	Array of $\sin\alpha$, (see Fig. 1.10)
BRO(I)	Array of stream channel normal thickness corresponding to the AMM(I) array, (m)
UTR(I,N)	Transformation parameter ($\equiv \frac{\partial X}{\partial \eta}$) [Note: $\partial X = \frac{\partial m}{r}$]
VTR(I,N)	Transformation parameter ($\equiv \frac{\partial Y}{\partial \eta}$) [Note: $dY = d\phi$]
VIC(I,N)	Transformation parameter ($\equiv \frac{\partial X}{\partial \xi}$)
UIC(I,N)	Transformation parameter ($\equiv \frac{\partial Y}{\partial \xi}$)
THETA(I,N)	Array of ϕ coordinate at each mesh point.

Instructions for Preparing Input

Units of Measurements:

The International System of Units is used throughout this report. The program does not use any constants which depend on the system of units being used. Therefore any consistent set of units may be used in preparing the input for the program. However, the angles must be supplied in degrees unless indicated otherwise, and the rotational speed is given in revolutions per second. Since any consistent set of units can be used, the output is not labeled with any units. In the examples supplied, the International System of Units are used.

Stream Surface Geometry:

The stream surface on which the flow is being determined, is a surface of revolution. Hence it is sufficient to define the mean stream surface of revolution (as seen in meridional plane, Fig. 1.9a). The stream surface required for the analysis is generated from the solution of a nonviscous version of the Navier-

Stokes equation as suggested by Wu [6]. The mean stream surface is defined by a set of m-coordinates and corresponding arrays of radii, sine of the angle made by the m-coordinate to the machine axis and the stream thickness for each 'm'.

Inlet and Outlet Flow Angles:

The value of β_{inlet} is given as an average value on AN. The exit flow angle β_{exit} is found iteratively. Normally one or two trial runs of the program are required to arrive at the exit flow angle. The iterative procedure is as follows. Estimated exit flow angle, β_{exit}, along GH is used to specify the values of stream function derivatives in the m-direction through the following relation

$$\frac{\partial\psi}{\partial m} = \frac{1}{2\pi/z} \frac{\tan\beta_{exit}}{\gamma_{exit}} \tag{1.1}$$

The flow field equations are then solved for the boundary function ψ given by equation (1.1) to obtain the velocity and pressure distribution throughout the stream annulus S_1 of Fig. 1.7. An evaluation of the torque developed by the annulus is obtained through the integration of the pressure and shear forces acting on the blade surfaces. The change in the annulus momentum between the known inlet and the estimated exit flow conditions is determined. If now the value of the predicted torque is not equal to the rate of change of the angular momentum, then the direction of the exit flow velocity is altered. The whole procedure is repeated until a satisfactory result is obtained.

Defining the Mesh:

A finite-difference mesh is used for the solution of the basic differential equation. A typical mesh pattern is shown in Fig. 1.11. The mesh spacing and the extent of the upstream and downstream regions are determined by the values of MXBI, MXBO and MX of the input. The program is presently set up to accept a maximum of 30 for MX. This is not a necessary constraint, the limit can be changed with very little effort. The values of MXBI, MXBO and MX should be determined such that the mesh which results has blocks which are approximately square. To achieve this, a value for NBBI is first chosen arbitrarily (15 to 20 typical). NBBI is a number of mesh spaces spanning the blade pitch S, where S = 2π/BLADE. Dividing S by NBBI gives the mesh spacing DN in the θ-direction in radians. Multiplying DN by an average radius (RIN) of the stream channel gives an average value of the actual mesh spacing in θ-direction. The value of axial chord of the blade should then be used with this tangential mesh spacing to calculate the approximate number of mesh spaces along the blade in the m-direction. This will give MXBO once MXBI is chosen.

Format for Input Data:

All the numbers on the first and second cards (Fig. 1.8) beginning with AMU and BTI respectively are real numbers (punch decimal point) in a 10-column field. The numbers on the third card beginning with MXBI are integers (no decimal point) in a five-column field (Fig. 1.8). And finally, all other numbers following the fourth card are real numbers specified in E format in a 14-column field.

Output

A sample output is shown in Table 1.1 for the radial inflow turbine rotor example. Since the complete output would be lengthy, only the first few lines of each section of output are reproduced here. Each section of the sample output in Table 1.1 has been numbered to correspond to the following description:

(1) The first output is an echo of the input data from Fig. 1.8. This comprises of sections (1a) and (1c). Though (1b) is not strictly an echo of the input data, it is useful for the future correction of the input data as explained in the section, Defining the Mesh. This is a printout of DS and DN, the grid spacing in the m-direction and θ-direction, respectively.

(2) This is the output which consists of blade transformation parameters. The output is displayed for each mesh point and begins from the line of constant η = 1 till the last η.

(3) These are the mean relative velocity at the inlet (WMIN) and the inlet Reynolds number.

(4) This is the maximum iteration required, the maximum values of the stream function, and the maximum value of the vorticity in the flow field.

(5) The values of the stream function, the meridional velocity, the tangential velocity, the vorticity and the pressure coefficient are displayed for each mesh point. These quantities are presented in groups along constant η lines.

1.3. PROGRAM PROCEDURE

The program is segmented into seven main parts, the subroutines VORT, STREAM, STAPRD, STORE, TEMP, CONVERG and subroutine function SPLINE are called by the main program. All the subroutines and their relations are shown in figure below. All information which must be transmitted between the seven main subroutines is placed in COMMON.

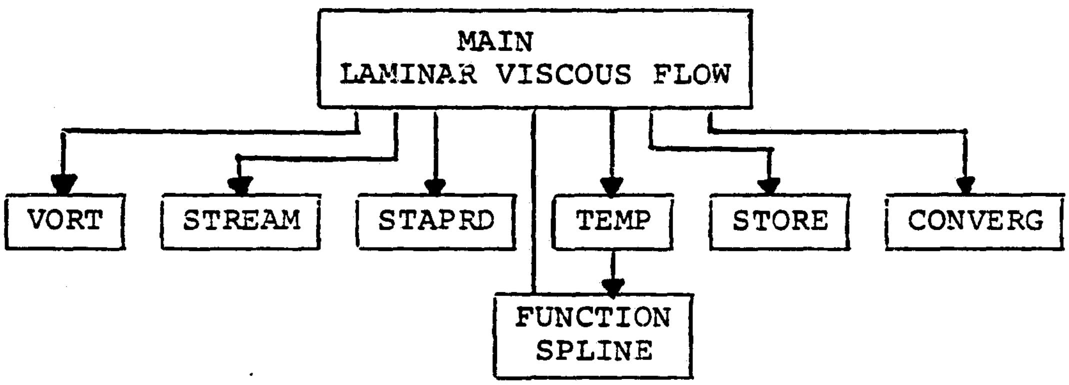

Fig. 1.12. Calling Relations of Subroutines.

The program was run on AMDAHL 470/V6-11 central processing unit with six magabytes real data storage. The program is presently set up to handle 30 by 40 mesh points; this was chosen to keep the running time reasonable. If, however, the user needs to use more mesh points, or if there is a storage problem on the user's computer, the maximum number of mesh points can be increased or reduced as the case may be by appropriately altering the dimension and common statements.

TABLE 1.1. INPUT DATA CARD LISTING.

RUN NO. 1 INPUT DATA CARD LISTING

1a

AMU	PRDNO	TIP	TBLADE	RHOIP	WTFL	OMEGA
.1709000D-04	.8000000	1083.000	500.0000	1.006000	.3200000D-02	4030.000
BTI	BTO	BLADE	BIN	RTIP	RIN	
-69.15000	-63.00030	11.00000	.9600000D-03	.7645000D-01	.8700000D-01	

MXBI	MXBO	MX	NBBI	ITRM	IPRINT	
4	33	19	30	-1	450	1

1b

DS	DN
0.0469510	0.0196920

1c

AMM	RADIUS	SAL	RRO
-0.007079	0.087000	-1.004280	0.000967
-0.007079	0.083527	-1.004280	0.000967
-0.003684	0.080123	-1.000120	0.000956
0.0	0.076450	-0.993984	0.000960
0.003498	0.072986	-0.985732	0.000982
0.006853	0.069697	-0.974760	0.001013
0.010048	0.066603	-0.960602	0.001043
0.013104	0.063701	-0.937357	0.001068
0.016034	0.060999	-0.904973	0.001090
0.018845	0.058511	-0.862745	0.001110
0.021535	0.056258	-0.810406	0.001128
0.024127	0.054236	-0.749061	0.001144
0.026630	0.052443	-0.681938	0.001156
0.029055	0.050874	-0.610477	0.001160
0.031413	0.049519	-0.540900	0.001155
0.033711	0.048348	-0.478504	0.001157
0.035959	0.047338	-0.420336	0.001179
0.038162	0.046477	-0.360370	0.001216
0.040329	0.045762	-0.299578	0.001253
0.042466	0.045177	-0.250202	0.001284
0.044574	0.044690	-0.21[illegible]78	0.001310
0.046662	0.044266	-0.19[illegible]22	0.001335
0.048730	0.043881	-0.180691	0.001362
0.050782	0.043516	-0.176406	0.001389
0.052817	0.043155	-0.179872	0.001416
0.054835	0.042782	-0.190020	0.001441
0.056835	0.042392	-0.200095	0.001465
0.058816	0.041987	-0.208736	0.001490
0.060776	0.041570	-0.215980	0.001514
0.062717	0.041145	-0.220585	0.001540
0.064639	0.040729	-0.209999	0.001568
0.066544	0.040353	-0.181434	0.001595
0.068434	0.040051	-0.135325	0.001620
0.070308	0.039843	-0.088592	0.001642
0.072176	0.039709	-0.057745	0.001660
0.074039	0.039618	-0.042105	0.001673
0.075898	0.039550	-0.031892	0.001681
0.077754	0.039499	-0.023363	0.001686
0.079607	0.039462	-0.016506	0.001688

TABLE 1.1 (Continued)

BLADE TRANSFORMATION PARAMETERS

MERD.COORD.	THETA	UTR	VTR	VIC	UIC	ALF	BFD	GAM	JAC
LINE OF CONST. ETA 1									
-0.007079	0.0	0.0	1.000000	1.000000	0.0	1.000000	0.0	1.000000	1.000000
-0.007079	0.0	0.0	1.000000	1.000000	0.0	1.000000	0.0	1.000000	1.000000
-0.003684	0.0	0.0	1.000000	1.000000	0.0	1.000000	0.0	1.000000	1.000000
0.0	0.0	0.0	1.000000	1.000000	0.0	1.000000	0.0	1.000000	1.000000
0.003458	0.0	0.0	1.000000	1.000000	0.0	1.000000	0.0	1.000000	1.000000
0.006853	0.0	0.0	1.000000	1.000000	0.0	1.000000	0.0	1.000000	1.000000
0.010048	0.0	0.0	1.000000	1.000000	0.0	1.000000	0.0	1.000000	1.000000
0.013104	0.0	0.0	1.000000	1.000000	0.0	1.000000	0.0	1.000000	1.000000
0.016034	0.0	0.0	1.000000	1.000000	0.0	1.000000	0.0	1.000000	1.000000
0.018845	0.0	0.0	1.000000	1.000000	0.0	1.000000	0.0	1.000000	1.000000
0.021535	0.0	0.0	1.000000	1.000000	0.0	1.000000	0.0	1.000000	1.000000
0.024127	0.0	0.0	1.000000	1.000000	0.0	1.000000	0.0	1.000000	1.000000
0.026630	0.0	0.0	1.000000	1.000000	0.0	1.000000	0.0	1.000000	1.000000
0.029055	0.0	0.0	1.000000	1.000000	0.0	1.000000	0.0	1.000000	1.000000
0.031413	0.0	0.0	1.000000	1.000000	0.0	1.000000	0.0	1.000000	1.000000
0.033711	0.0	0.0	1.000000	1.000000	0.0	1.000000	0.0	1.000000	1.000000
0.035959	0.0	0.0	1.000000	1.000000	0.0	1.000000	0.0	1.000000	1.000000
0.038162	0.0	0.0	1.000000	1.000000	0.0	1.000000	0.0	1.000000	1.000000
0.040329	0.0	0.0	1.000000	1.000000	0.0	1.000000	0.0	1.000000	1.000000
0.042466	0.0	0.0	1.000000	1.000000	0.0	1.000000	0.0	1.000000	1.000000
0.044574	0.0	0.0	1.000000	1.000000	0.0	1.000000	0.0	1.000000	1.000000
0.046662	0.0	0.0	1.000000	1.000000	0.0	1.000000	0.0	1.000000	1.000000
0.048730	0.0	0.0	1.000000	1.000000	0.0	1.000000	0.0	1.000000	1.000000
0.050782	0.0	0.0	1.000000	1.000000	0.0	1.000000	0.0	1.000000	1.000000
0.052817	0.0	0.0	1.000000	1.000000	0.0	1.000000	0.0	1.000000	1.000000
0.054835	0.0	0.0	1.000000	1.000000	0.0	1.000000	0.0	1.000000	1.000000
0.056835	0.0	0.0	1.000000	1.000000	0.0	1.000000	0.0	1.000000	1.000000
0.058816	0.0	0.0	1.000000	1.000000	0.0	1.000000	0.0	1.000000	1.000000
0.060776	0.0	0.0	1.000000	1.000000	0.0	1.000000	0.0	1.000000	1.000000
0.062717	0.0	0.0	1.000000	1.000000	0.0	1.000000	0.0	1.000000	1.000000
0.064639	0.0	0.0	1.000000	1.000000	0.0	1.000000	0.0	1.000000	1.000000
0.066544	0.0	0.0	1.000000	1.000000	0.0	1.000000	0.0	1.000000	1.000000
0.068434	0.0	0.0	1.000000	1.000000	0.0	1.000000	0.0	1.000000	1.000000
0.070308	0.0	0.0	1.000000	1.000000	0.0	1.000000	0.0	1.000000	1.000000
0.072176	0.0	0.0	1.000000	1.000000	0.0	1.000000	0.0	1.000000	1.000000
0.074039	0.0	0.0	1.000000	1.000000	0.0	1.000000	0.0	1.000000	1.000000
0.075898	0.0	0.0	1.000000	1.000000	0.0	1.000000	0.0	1.000000	1.000000
0.077754	0.0	0.0	1.000000	1.000000	0.0	1.000000	0.0	1.000000	1.000000
0.079607	0.0	0.0	1.000000	1.000000	0.0	1.000000	0.0	1.000000	1.000000
LINE OF CONST. ETA 2									
-0.007079	0.0	0.0	1.000000	1.000000	0.0	1.000000	0.0	1.000000	1.000000
-0.007079	0.0	0.0	1.000000	1.000000	0.0	1.000000	0.0	1.000000	1.000000
-0.003684	0.0	0.0	1.000000	1.000000	0.0	1.000000	0.0	1.000000	1.000000
0.0	0.0	0.0	1.000000	1.000000	0.0	1.000000	0.0	1.000000	1.000000
0.003458	0.0	0.0	1.000000	1.000000	0.0	1.000000	0.0	1.000000	1.000000
0.006853	0.0	0.0	1.000000	1.000000	0.0	1.000000	0.0	1.000000	1.000000
0.010048	0.0	0.0	1.000000	1.000000	0.0	1.000000	0.0	1.000000	1.000000
0.013104	0.0	0.0	1.000000	1.000000	0.0	1.000000	0.0	1.000000	1.000000
0.016034	0.0	0.0	1.000000	1.000000	0.0	1.000000	0.0	1.000000	1.000000
0.018845	0.0	0.0	1.000000	1.000000	0.0	1.000000	0.0	1.000000	1.000000
0.021535	0.0	0.0	1.000000	1.000000	0.0	1.000000	0.0	1.000000	1.000000
0.024127	0.0	0.0	1.000000	1.000000	0.0	1.000000	0.0	1.000000	1.000000
0.026630	0.0	0.0	1.000000	1.000000	0.0	1.000000	0.0	1.000000	1.000000
0.029055	0.0	0.0	1.000000	1.000000	0.0	1.000000	0.0	1.000000	1.000000
0.031413	0.0	0.0	1.000000	1.000000	0.0	1.000000	0.0	1.000000	1.000000
0.033711	0.0	0.0	1.000000	1.000000	0.0	1.000000	0.0	1.000000	1.000000
0.035959	0.0	0.0	1.000000	1.000000	0.0	1.000000	0.0	1.000000	1.000000
0.038162	0.0	0.0	1.000000	1.000000	0.0	1.000000	0.0	1.000000	1.000000
0.040329	0.0	0.0	1.000000	1.000000	0.0	1.000000	0.0	1.000000	1.000000
0.042466	0.0	0.0	1.000000	1.000000	0.0	1.000000	0.0	1.000000	1.000000
0.044574	0.0	0.0	1.000000	1.000000	0.0	1.000000	0.0	1.000000	1.000000
0.046662	0.0	0.0	1.000000	1.000000	0.0	1.000000	0.0	1.000000	1.000000
0.048730	0.0	0.0	1.000000	1.000000	0.0	1.000000	0.0	1.000000	1.000000
0.050782	0.0	0.0	1.000000	1.000000	0.0	1.000000	0.0	1.000000	1.000000
0.052817	0.0	0.0	1.000000	1.000000	0.0	1.000000	0.0	1.000000	1.000000
0.054835	0.0	0.0	1.000000	1.000000	0.0	1.000000	0.0	1.000000	1.000000
0.056835	0.0	0.0	1.000000	1.000000	0.0	1.000000	0.0	1.000000	1.000000
0.058816	0.0	0.0	1.000000	1.000000	0.0	1.000000	0.0	1.000000	1.000000
0.060776	0.0	0.0	1.000000	1.000000	0.0	1.000000	0.0	1.000000	1.000000
0.062717	0.0	0.0	1.000000	1.000000	0.0	1.000000	0.0	1.000000	1.000000
0.064639	0.0	0.0	1.000000	1.000000	0.0	1.000000	0.0	1.000000	1.000000
0.066544	0.0	0.0	1.000000	1.000000	0.0	1.000000	0.0	1.000000	1.000000
0.068434	0.0	0.0	1.000000	1.000000	0.0	1.000000	0.0	1.000000	1.000000
0.070308	0.0	0.0	1.000000	1.000000	0.0	1.000000	0.0	1.000000	1.000000
0.072176	0.0	0.0	1.000000	1.000000	0.0	1.000000	0.0	1.000000	1.000000
0.074039	0.0	0.0	1.000000	1.000000	0.0	1.000000	0.0	1.000000	1.000000
0.075898	0.0	0.0	1.000000	1.000000	0.0	1.000000	0.0	1.000000	1.000000
0.077754	0.0	0.0	1.000000	1.000000	0.0	1.000000	0.0	1.000000	1.000000
0.079607	0.0	0.0	1.000000	1.000000	0.0	1.000000	0.0	1.000000	1.000000
LINE OF CONST. ETA 3									
-0.007079	0.0	0.0	1.000000	1.000000	0.0	1.000000	0.0	1.000000	1.000000

2

PART II

2.1. NUMERICAL EXAMPLE

The equations formulated in Volume II [7] are programmed for numerical solution using the finite difference technique. The program is arranged to handle general flow within turbomachinery, which may be of the axial, radial or mixed flow type. To illustrate the use of the method of analysis a sample problem will be discussed. The input and output of the program will be presented.

Nonadiabatic Flow in a Mixed Flow Turbine

The versatility of the present method of solution is predicting the behavior of the viscous nonadiabatic flow in turbomachinery is demonstrated by analyzing the flow in a cooled mixed-flow turbine rotor. The rotor geometry is shown in Fig. 2.1 together with the shape and thickness distribution of the mid-channel stream annulus, S_1. The blade-to-blade shape in the physical domain as well as the boundary fitted coordinates employed in the solution are shown in Figs. 2.2 and 2.3. Additional summary data related to the blades geometry and the configuration of stream annulus S_1 can be found in Table 2.1. The following operating conditions which correspond to the design point of the turbine are used in the analysis. The program output is presented in Tables 2.2 and 2.3.

Turbine inlet total temperature, T_t, 1083°K
Turbine inlet density, ρ, 1.0060 Kg/m^3
Mass flow per blade for the stream annulus, $\dot{M}$, 0.00320 Kg/sec
Rotational speed, Ω, 38,500 rpm
Inlet flow angke, β_{in} (see Fig. 1.10), 62.5°
Exit flow angle, β_{exit} (see Fig. 1.10), 63°
Meridional component of the relative velocity at rotor inlet, W_m, 66.2 m/s
Flow Reynolds number at rotor inlet, Re $\left(\equiv \frac{\rho W_m r_{tip}}{\mu_e}\right)_{inlet}$, 3.34×10^5
Prandtl number, 0.8
Working fluid, air.

12

The results are presented in Figs. 2.4 through 2.9 as contour plots for the distribution of the stream function, the velocity, the kinetic energy of turbulence, the static pressure as well as the temperature within the blade passages. The detailed discussion of these results will be found in reference [7].

2.2. DESCRIPTION OF INPUT AND OUTPUT FOR TURBULENT VISCOUS FLOW PROBLEM

The program requires as an input the configuration of the stream channel annulus S_1, the inlet flow conditions, the rotational speed of the machine, and the blade geometry. Recalling that all the flow calculations are carried out in the unit square of the transformed domain, therefore the blade input geometry is supplied to the program in the form of the transformation parameters δ, β, γ and J. As pointed out in reference [1], these parameters may be specified for any blade geometry using Thompson code for the automatic numerical generation of boundary fitted coordinate system [13].

The program output consists of the distribution of the stream function, the vorticity, the kinetic energy of turbulence, its dissipation rate, and the static pressures within the blade passages. The variation of meridional and tangential velocity components from blade-to-blade and from the inlet of the machine to its exit are also generated. In cases where blade cooling is considered, the program has the capability to generate the temperature distribution within the blade passages. In order to keep the computer time within reasonable limits, (usually less than 5 minutes on an ANDAHL 470), the flow domain has been divided, for all calculations, into 30 step sizes in η direction and 40 in the ζ direction, with the greater number of nodes distributed in the meridional direction.

Input

The description of the input variable, the input form (Fig. 1.8) and their formats are presented in Part I of this report and are valid for the turbulent program. Also the comments made about Units of Measurements, Stream Surface Geometry, Inlet and Outlet Flow Angles, and Defining the Mesh, in the section, "Instructions for Preparing Input," of Part I hold good for the turbulent program presented here in Part II.

Output

However, the output for the turbulent program needs some more explaining. The sample output is shown in Table 2.2 and Table 2.3. Here again, since the complete output would be lengthy only parts of all relevant output are reproduced in the two Tables 2.2 and 2.3. Each section of the sample output in Table 2.2 and Table 2.3 are sequentially numbered in subdivisions to correspond to the following description:

(1) The first output is an echo of the input data. This comprises of sections (1a) and (1c). The output in section (1a) is identically described in Fig. 1.8. Section (1c) displays the blade geometry data. Though section (1b) is not an echo of the data, it is an important derived quantity DS and DN, the mesh spacings. These are displayed to help adjust the mesh size.

(2) This is the output which echoes the blade transformation parameters. The output is displayed for each mesh point, and begins from the line of constant $\eta = 1$ till the last η.

(3) These are the mean relative velocity at the inlet, the Reynolds number at the inlet, and two intermediate parameters.

(4) This is the maximum iteration required, the maximum value of vorticity, the maximum value of the stream function, the maximum value of kinetic energy of turbulence, and the maximum value of dissipation function.

(5) Finally, the values of stream function, meridional velocity, tangential velocity, vorticity, kinetic energy of

turbulence, dissipation energy, Reynolds number and pressure coefficient are displayed for each mesh point. These quantities are presented in groups along constant η lines.

2.3. PROGRAM PROCEDURE

The program is segmented into ten main parts, the subroutines, VORT, STREAM, ENERGY, DSPAT, TEMP, STAPRS, STORE, CONVRG and subroutine function SPLINE are called by the main program. All the subroutines and their relation are shown in figure below. All information which must be transmitted between the ten main subroutines is placed in COMMON.

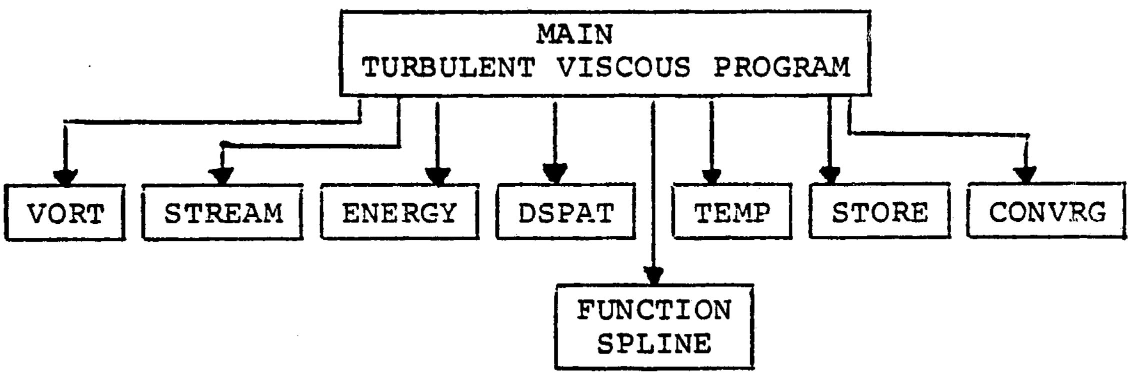

Fig. 2.10. Calling Relation of Subroutines.

TABLE 2.1 BLADE GEOMETRY DATA FOR THE MIXED FLOW TURBINE

Blade Upper Surface Data

Meridional Distance m(m)	Angular Coordinate ϕ	Derivative	2nd Derivative
0.625390D-03	0.56273	-0.45676	-7.2554
0.860000D-02	0.55900	-0.46035	6.3594
0.160000D-01	0.55560	-0.48120	-11.995
0.235000D-01	0.55220	-0.35261	46.288
0.290300D-01	0.55050	-0.34501	-43.542
0.342800D-01	0.54900	-0.528140D-01	154.06
0.395400D-01	0.54640	-1.7845	-813.31
0.462300D-01	0.51540	-7.6118	-928.77
0.539400D-01	0.42000	-15.962	-1242.5
0.619700D-01	0.23630	-33.644	-3206.4
0.670110D-01	0.238560D-01	-50.743	-3497.8

Blade Lower Surface Data

Meridional Distance m(m)	Angular Coordinate ϕ	Derivative	2nd Derivative
0.625390D-03	0.847100D-02	0.45678	5.7000
0.860000D-02	0.122000D-01	0.46655	-3.2487
0.160000D-01	0.156000D-01	0.45729	0.74568
0.235000D-01	0.169000D-01	0.40262	-15.325
0.290300D-01	0.209000D-01	0.32213	-13.787
0.342800D-01	0.215000D-01	-0.26520	-209.96
0.395400D-01	0.160000D-01	-2.0543	-470.30
0.462300D-01	-0.116000D-01	-6.6949	-917.03
0.539400D-01	-0.962000D-01	-15.993	-1495.0
0.619700D-01	-0.27910	-30.342	-2078.9
0.623630D-01	-0.53070	-50.743	-4303.7

TABLE 2.2. INPUT DATA CARD LISTING.

1a

RUN NO. 1 INPUT DATA CARD LISTING

AMU	PRONU	TIP	TBLADE	RHOIP	WIFL	OMEGA
.1790000D-04	1.000000	2200.000	600.0000	.3950000	.12680000-02	4930.000
BTI	BTO	BLADE	BIN	RTIP	RIN	
-54.00000	-63.00000	11.00000	.96700000-03	.76450000-01	.87000000-01	

MXBI	MXBO	MX	NOBI	ITRB	IPRINT
4	33	39	30	-1	50

1b

DS	DN
0.0263158	0.0311834

1c

AMM	RADIUS	SAL	BRO
-0.007079	0.087000	-1.004280	0.000967
-0.007079	0.083527	-1.004280	0.000967
-0.003684	0.080123	-1.000120	0.000956
0.0	0.076450	-0.993984	0.000960
0.003498	0.072986	-0.985732	0.000982
0.006853	0.069697	-0.974760	0.001013
0.010048	0.066603	-0.960602	0.001043
0.013104	0.063701	-0.937357	0.001068
0.016034	0.060999	-0.904973	0.001090
0.018845	0.058511	-0.862745	0.001110
0.021535	0.056258	-0.810406	0.001128
0.024127	0.054236	-0.749061	0.001144
0.026630	0.052443	-0.681938	0.001156
0.029055	0.050874	-0.610477	0.001160
0.031413	0.049519	-0.540900	0.001155
0.033711	0.048348	-0.478504	0.001157
0.035959	0.047338	-0.420336	0.001179
0.038162	0.046477	-0.360370	0.001216
0.040329	0.045762	-0.299578	0.001253
0.042466	0.045177	-0.250202	0.001284
0.044574	0.044690	-0.214878	0.001310
0.046662	0.044266	-0.192922	0.001335
0.048730	0.043881	-0.180691	0.001362
0.050782	0.043516	-0.176406	0.001389
0.052817	0.043155	-0.179872	0.001416
0.054835	0.042782	-0.190020	0.001441
0.056835	0.042392	-0.200095	0.001465
0.058816	0.041987	-0.208736	0.001490
0.060776	0.041570	-0.215980	0.001514
0.062717	0.041145	-0.220585	0.001540
0.064639	0.040729	-0.209999	0.001568
0.066544	0.040353	-0.181434	0.001595
0.068434	0.040051	-0.135325	0.001620
0.070308	0.039843	-0.088592	0.001642
0.072176	0.039709	-0.057745	0.001660
0.074039	0.039618	-0.042105	0.001673
0.075898	0.039550	-0.031892	0.001681
0.077754	0.039499	-0.023363	0.001686
0.079607	0.039462	-0.016506	0.001688

TABLE 2.2 (Continued)

BLADE TRANSFORMATION PARAMETERS

MERD. COORD.	THETA	UTR	VTR	VIC	UIC	ALF	BFD	GAH	JAC
LINE OF CONST. ETA 1									
-0.007079	0.571178	0.0	0.571209	1.785220	-0.000036	0.326789	-0.000021	3.187046	1.019739
-0.007079	0.571199	0.0	0.571762	1.785220	-0.000009	0.326912	-0.000005	3.187910	1.020721
-0.003684	0.571198	0.000001	0.571762	1.785220	0.0	0.326912	0.000002	3.187910	1.020721
0.0	0.571199	0.000000	0.573062	1.785220	0.185596	0.328409	0.106258	3.221456	1.023942
0.003498	0.561436	-0.000001	0.551295	1.785220	0.215074	0.303726	0.119119	3.233698	0.984183
0.006853	0.559413	0.0	0.549068	1.785220	0.059954	0.301476	0.032425	3.190498	0.980207
0.010048	0.554330	0.0	0.546026	1.785230	0.055010	0.298144	0.030037	3.190072	0.974782
0.013104	0.556940	0.0	0.543232	1.785220	0.052340	0.295101	0.028437	3.189750	0.969789
0.016034	0.555577	0.0	0.540536	1.785220	0.051022	0.292179	0.028012	3.189696	0.964976
0.018845	0.554214	0.0	0.537908	1.785230	0.049313	0.289345	0.026526	3.189478	0.960289
0.021535	0.552933	0.0	0.535405	1.785230	0.042093	0.286659	0.022537	3.188818	0.955821
0.024127	0.552000	0.0	0.533358	1.785220	0.033280	0.284471	0.017759	3.188118	0.952161
0.026630	0.551232	-0.000014	0.531754	1.785220	0.029028	0.282762	0.015411	3.187853	0.949298
0.029055	0.551471	0.0	0.530164	1.785230	0.029669	0.281074	0.015729	3.187926	0.946465
0.031413	0.549672	-0.000014	0.528684	1.785220	0.025710	0.279507	0.013568	3.187707	0.943921
0.033711	0.549120	0.0	0.528103	1.785220	0.015280	0.278893	0.008069	3.187244	0.942789
0.035959	0.548868	0.0	0.528908	1.785220	0.023035	0.279828	0.012185	3.187541	0.944369
0.038162	0.547909	0.0	0.530482	1.785230	0.082271	0.281411	0.043643	3.193815	0.947032
0.040329	0.544541	-0.000014	0.531367	1.785230	0.195952	0.282351	0.104098	3.225443	0.948615
0.042466	0.537602	-0.000014	0.530758	1.785220	0.343247	0.281794	0.182156	3.304829	0.947525
0.044574	0.525486	-0.000014	0.529030	1.785220	0.494695	0.279873	0.261684	3.431724	0.944443
0.046662	0.511581	-0.0	0.527135	1.785230	0.641280	0.277871	0.338041	3.598286	0.941957
0.048720	0.492755	0.0	0.525406	1.785230	0.794724	0.276051	0.417553	3.818632	0.937971
0.050762	0.469778	0.0	0.523996	1.785220	0.956937	0.274572	0.501431	4.102739	0.935440
0.052817	0.442429	-0.000014	0.523277	1.785210	1.170700	0.273819	0.591387	4.464327	0.934175
0.054836	0.413329	-0.0	0.523180	1.785210	1.322150	0.273717	0.691722	4.936055	0.933986
0.056835	0.372875	0.0	0.523512	1.785240	1.568060	0.274065	0.820898	5.645894	0.934595
0.058816	0.327850	0.000041	0.522931	1.785240	1.897100	0.273457	0.992126	6.786070	0.933479
0.060776	0.273087	0.000041	0.519515	1.785220	2.272630	0.269896	1.180739	8.351858	0.927354
0.062717	0.208309	0.0	0.512907	1.785220	2.669480	0.263074	1.369195	10.313134	0.915652
0.064639	0.132673	0.0	0.503727	1.785220	3.086330	0.253741	1.554668	12.712443	0.899264
0.066544	0.045968	0.0	0.494471	1.785220	3.500200	0.244502	1.720747	15.438410	0.882740
0.068434	-0.051438	0.0	0.486438	1.785220	3.688940	0.236622	1.794441	16.795289	0.868397
0.070308	-0.140070	0.0	0.492854	1.785220	3.667500	0.242995	1.807542	16.637567	0.879951
0.072176	-0.241349	0.0	0.494484	1.785220	3.655080	0.244514	1.807774	16.552469	0.882763
0.074039	-0.340170	0.0	0.494553	1.785220	3.647240	0.244583	1.803753	16.489370	0.882986
0.075898	-0.436194	0.0	0.494567	1.785220	3.640520	0.244597	1.800481	16.440396	0.882911
0.077754	-0.531961	-0.0	0.494553	1.785220	3.635260	0.244583	1.797829	16.402126	0.882986
0.079607	-0.627409	0.0	0.494733	1.785220	3.630710	0.244761	1.796237	16.369066	0.883207
LINE OF CONST. ETA 2									
-0.007079	0.551502	0.0	0.571238	1.785230	0.000725	0.326313	0.000414	3.187047	1.019791
-0.007079	0.551489	0.0	0.571453	1.785220	0.000239	0.326559	0.000137	3.187011	1.020167
-0.003684	0.551489	0.0	0.571453	1.785220	0.000544	0.326559	0.000311	3.187011	1.020169
0.0	0.551461	0.000000	0.571816	1.785220	0.173392	0.326974	0.098577	3.216729	1.020817
0.003498	0.542422	0.0	0.551620	1.785220	0.200633	0.304285	0.110673	3.227264	0.984763
0.006853	0.549908	0.0	0.548701	1.785220	0.055379	0.301071	0.030787	3.190077	0.979552
0.010048	0.539509	0.0	0.545678	1.785230	0.051195	0.297764	0.027976	3.189667	0.974161
0.013104	0.538215	0.0	0.542881	1.785220	0.048740	0.294720	0.026460	3.189386	0.969162
0.016034	0.536945	0.0	0.540186	1.785220	0.048325	0.291801	0.026105	3.189346	0.964351
0.018845	0.535673	0.0	0.537547	1.785230	0.045973	0.290957	0.024712	3.189160	0.959645
0.021535	0.534527	0.0	0.535132	1.785230	0.039141	0.286766	0.020945	3.188578	0.955334
0.024127	0.533614	0.0	0.533084	1.785220	0.030849	0.284179	-0.016445	3.187962	0.951672
0.026630	0.532904	0.0	0.531381	1.785220	0.026906	0.282366	0.014297	3.187734	0.948637
0.029055	0.532199	0.0	0.529807	1.785230	0.027690	0.280695	0.014679	3.187813	0.945927
0.031413	0.531449	0.0	0.528414	1.785220	0.024388	0.279221	0.012887	3.187605	0.943335
0.033711	0.530916	0.000001	0.527941	1.785220	0.015478	0.278616	0.008151	3.187249	0.942312
0.035959	0.530636	0.0	0.528578	1.785220	0.024537	0.279395	0.012969	3.187612	0.943624
0.038162	0.529625	0.000001	0.530029	1.785220	0.083766	0.280930	0.044400	3.194027	0.946217
0.040329	0.526329	0.000001	0.530755	1.785230	0.196060	0.281701	0.104061	3.225486	0.947520
0.042466	0.519413	0.0	0.530088	1.785220	0.341707	0.280997	0.181135	3.303774	0.946324
0.044574	0.508256	0.000001	0.528405	1.785220	0.492377	0.279212	0.260155	3.429406	0.943319
0.046662	0.493416	0.000001	0.526516	1.785230	0.638910	0.277219	0.336398	3.595252	0.939957
0.048720	0.474649	0.000001	0.524790	1.785230	0.792694	0.275405	0.415999	3.815410	0.936870
0.050782	0.451720	0.000001	0.523473	1.785220	0.955577	0.274024	0.500218	4.100128	0.934514
0.052817	0.424386	0.000001	0.522759	1.785210	1.129680	0.273277	0.590552	4.463152	0.933274
0.054835	0.392299	0.0	0.522680	1.785210	1.322290	0.273194	0.691135	4.935426	0.933994
0.056835	0.354833	0.0	0.522047	1.785220	1.567830	0.272474	0.819892	5.645101	0.933575
0.058816	0.309881	0.000014	0.522251	1.785220	1.894470	0.272746	0.989414	6.776927	0.932307
0.060776	0.255184	0.000014	0.519940	1.785240	2.266110	[illegible]	[illegible]	[illegible]	[illegible]

2

TABLE 2.3

WMIN = 66.287642 REYNOLD = 283111.187 SAL1 = -9.33544 SAL2 = 0.153437 3

ITER = 150 CCWM = -0.003470 CCSIM = 0.001864
ICOUNT = 50 CCEKM = -0.001369 CCDSPM = 0.001019 4

5

ST.FCT.	MER.VEL.	TAG.VEL.	VORT.	KE. TUR.	DISP.	RENOLD	PRES.COF.
LINE OF CONST. ETA 1							
0.0	24.88071	31.29915	36.84290	1.12488	0.03649	147063.63682	-0.23174
0.0	9.07220	1.09805	17.67217	0.67208	0.03994	181254.02645	-0.29875
0.0	4.79147	0.15850	11.39095	0.48566	0.03453	206547.42254	-0.38476
0.0	3.77498	0.11632	11.04505	0.54371	0.02898	197548.46663	-0.46306
0.0	3.65369	0.12712	12.36458	0.71217	0.04357	177062.50634	-0.53368
0.0	3.80818	0.11055	14.47089	0.98096	0.07043	155500.20667	-0.59708
0.0	4.19332	0.11583	17.34563	1.36450	0.11554	135899.52853	-0.65380
0.0	4.83225	0.11325	21.08022	1.89115	0.19853	118842.76442	-0.72475
0.0	5.65146	0.10535	25.75459	2.59695	0.30337	104241.87818	-0.74921
0.0	6.70649	0.10905	31.32181	3.52342	0.47944	91828.88496	-0.78991
0.0	7.84921	0.13045	37.45008	4.70607	0.74007	81374.77603	-0.82334
0.0	8.86633	0.12769	43.25033	6.14155	1.10332	72777.27209	-0.85270
0.0	9.55545	0.08178	47.85099	7.78668	1.57512	65856.93069	-0.87789
0.0	9.99381	0.12902	51.58662	9.67645	2.18202	60081.91220	-0.90952
0.0	10.59675	0.48835	56.12668	12.03855	3.02792	54771.66421	-0.92190
0.0	11.69121	1.28326	62.16928	15.26378	4.32292	49516.28779	-0.93911
0.0	13.33563	2.56406	73.90759	19.83749	6.40492	44281.44320	-0.95492
0.0	15.34682	4.25269	88.58787	26.25959	9.75474	39275.37141	-0.96921
0.0	17.40620	6.25255	106.52718	35.02495	15.02623	34708.15788	-0.98246
0.0	18.85447	8.39737	126.97066	46.68266	23.12156	30669.11019	-0.99449
0.0	18.18029	9.74524	147.71116	60.43045	34.05395	27433.81034	-1.00278
0.0	16.03441	10.15124	172.69585	76.18777	48.20717	24814.94153	-1.00736
0.0	12.48344	9.24540	207.32709	95.08929	67.21731	22539.39077	-1.00914
0.0	7.19696	6.32143	256.72186	120.80632	96.25388	20310.55530	-1.00427
0.0	-0.56806	-0.60366	327.40176	159.87385	146.53788	17974.56168	-0.98766
0.0	-11.21214	-14.27334	406.43424	213.66545	226.40458	15833.95764	-0.95978
0.0	-24.57051	-36.74084	462.58468	279.27728	338.32737	14080.45493	-0.92807
0.0	-33.20697	-67.78193	462.68198	347.82094	470.23757	12786.52628	-0.91512
0.0	-52.78751	-103.49807	374.23625	405.87403	592.74873	11947.17342	-0.98935
LINE OF CONST. ETA 2							
-0.00761	8.57362	15.53376	-7.77331	1.12488	0.01816	5592.73768	-0.20192
-0.00334	6.53262	3.37103	-1.09877	15.32211	1.60631	2843.68309	-0.29466
-0.00204	4.90719	0.94808	0.40750	10.84995	0.75808	2553.41751	-0.38304
-0.00168	4.41742	0.32714	0.67476	11.21753	0.71407	2253.05415	-0.46177
-0.00162	4.46624	0.12633	0.79816	13.42974	0.91833	2023.61702	-0.53245
-0.00167	4.79158	0.04280	0.99160	16.74698	1.27926	1814.26938	-0.59580
-0.00179	5.30067	-0.02412	1.15499	21.02529	1.89250	1622.93259	-0.65239
-0.00198	5.97054	-0.09994	1.26550	26.71886	2.52558	1452.06549	-0.70269
-0.00223	6.78595	-0.17283	1.27671	32.71126	3.49425	1301.16884	-0.74717
-0.00251	7.68929	-0.19459	1.14005	40.27990	4.75804	1169.00660	-0.78625
-0.00278	8.58401	-0.13877	0.88310	49.04624	6.36708	1055.50730	-0.82014
-0.00298	9.37301	-0.07616	0.67531	58.86771	8.35763	962.06795	-0.84886
-0.00313	10.00023	-0.09953	0.72457	69.55264	10.77346	888.62415	-0.87357
-0.00320	10.60548	-0.12393	1.02834	81.48374	13.80215	829.58115	-0.89599
-0.00357	11.40963	0.11035	1.32913	95.85558	17.86651	775.99213	-0.91591
-0.00400	12.57040	0.80123	1.33044	113.95783	23.51166	722.41796	-0.93307
-0.00455	13.99508	2.09464	0.86948	136.73612	31.23133	668.51501	-0.94713
-0.00515	15.41438	3.57957	-0.14907	164.88395	42.00196	616.17442	-0.95966
-0.00571	16.46949	5.30988	-1.82082	198.70672	56.20724	567.61379	-0.96814
-0.00602	16.66136	7.26897	-3.92190	237.36435	74.22988	525.22319	-0.97589
-0.00576	15.44719	8.84076	-4.40010	275.26592	94.35484	496.35379	-0.98192
-0.00501	12.94984	9.30570	-4.52930	312.55787	117.13426	477.85650	-0.98583
-0.00376	9.06276	8.44793	-4.38562	352.22799	144.88498	465.27121	-0.98783
-0.00186	3.37409	5.53055	-3.88014	399.79819	183.03980	455.27165	-0.98910
0.00094	-4.77152	-1.47599	-2.59369	462.68276	242.23157	459.72761	-0.98569
0.00476	-15.68756	-15.34382	-0.77102	533.07028	319.46848	447.65698	-0.98902
0.00943	-29.04396	-38.08561	1.18275	604.06219	412.52455	449.93926	-1.00323
0.01443	-43.75240	-69.98164	2.27023	662.55934	507.86120	460.15657	-1.03527
0.01954	-60.64956	-107.05743	-1.07797	697.63206	579.69137	473.44057	-1.11642

REFERENCES

1. Katsanis, T., "Use of Arbitrary Quasi-Orthogonals for Calculating Flow Distribution in the Meridional Plane of a Turbomachine," NASA TND-2546, December 1964.
2. Khalil, I. and Tabakoff, W., "A Calculation Procedure for Viscous Flow in Turbomachines - Vol. I," NASA CR 159635, July 1979.
3. Watanabe, I., Arigh, I. and Fujie, K., "A Study of the Flow Patterns in an Impeller Channel of a Radial Turbine," Trans. ASME, Journal of Engineering for Power, Oct. 1967, p. 467.
4. Benson, R.S., Cartwright, W.G. and Hill, M., "Analytical and Experimental Studies of Two-Dimensional Flows in a Radial Bladed Impeller," ASME Paper 71-GT-20, 1971.
5. Katsanis, T., "Fortran Program for Calculating Transonic Velocities on a Blade-to-Blade Stream Surface of a Turbomachine," NASA TN D-5427, 1969.
6. Wu, C.H., "A General Theory of Three-Dimensional Flow in Subsonic and Supersonic Turbomachines of Axial, Radial and Mixed Flow Types," National Advisory Committee for Aeronautics, NACA TN 2604, 1952.
7. Khalil, I. and Tabakoff, W., "A Calculation Procedure for Viscous Flow in Turbomachines - Vol. II," NASA CR 159636, January 1980.
8. Launder, B.E. and Spalding, D.B., "The Numerical Computations of Turbulent Flows," Computer Methods in Applied Mechanics and Engineering, Vol. 3, 1974, pp. 269-289.
9. Wilcox, D.C. and Chambers, T.L., "Critical Examination of Two-Equations Turbulence Closure Models," AIAA Paper No. 76-352, 1976.
10. Quemord, C. and Michel, R., "Definition and Application of Means for Predicting Shear Turbulent Flows in Turbomachines," ASME Paper 76-GT-67, 1976.
11. Dodge, P.R., "A Numerical Method for 2-D and 3-D Viscous Flow," AIAA Paper No. 76-425, 1976.

12. Roache, P.J., Computational Fluid Dynamics, Hermosa Publishers, Albuquerque, New Mexico, 1972.

13. Thompson, J.F., Thames, F.C. and Wayne, C., "Automatic Numerical Generation of Body-Fitted Curvilinear Coordinate System for Field Containing any Number of Arbitrary Two-Dimensional Bodies," Journal of Computational Physics, Vol. 15, 1974, pp. 299-319.

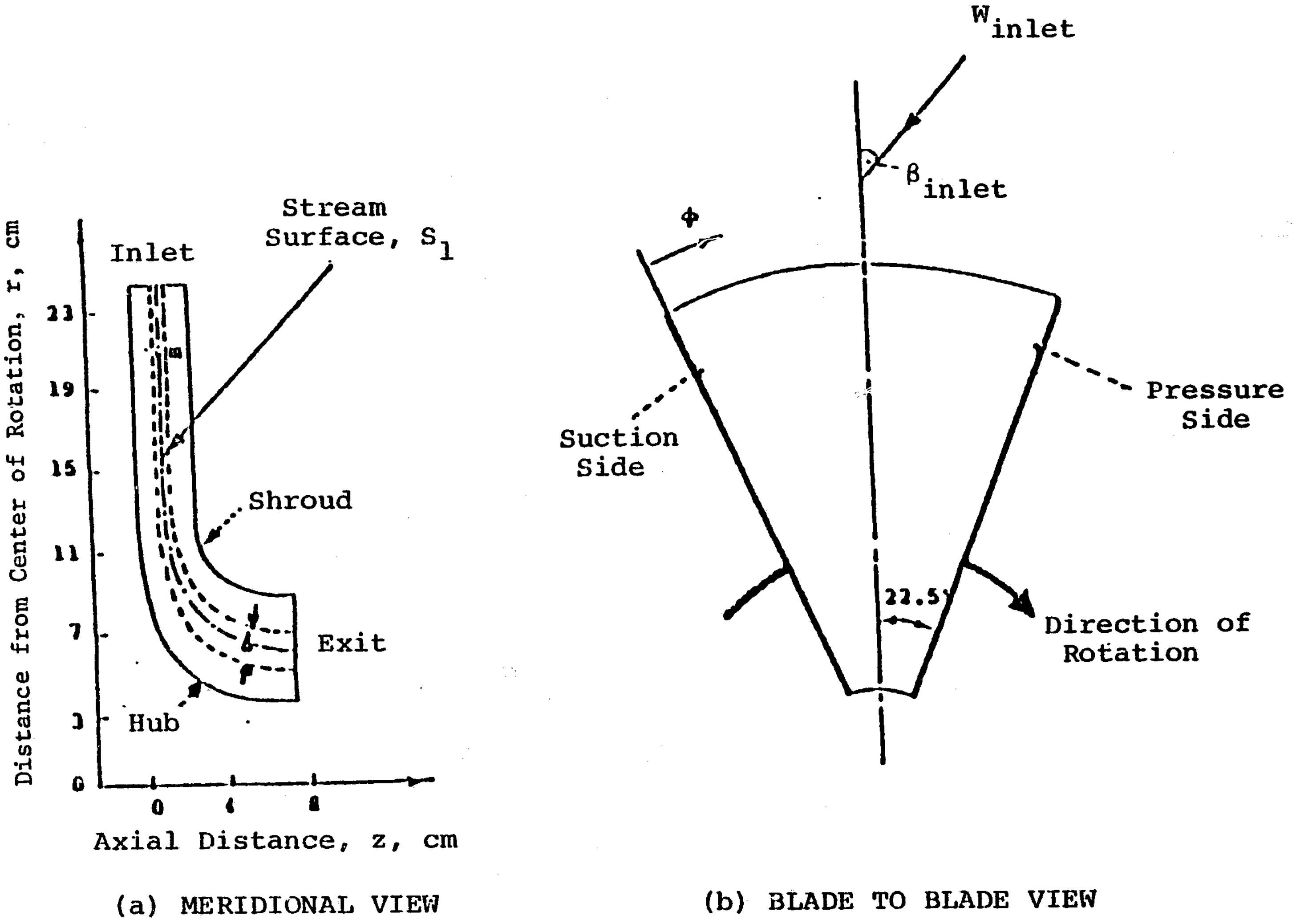

FIG. 1.1. HUB-SHROUD PROFILE WITH THE STREAM SURFACE S_1, USED FOR BLADE-TO-BLADE ANALYSIS.

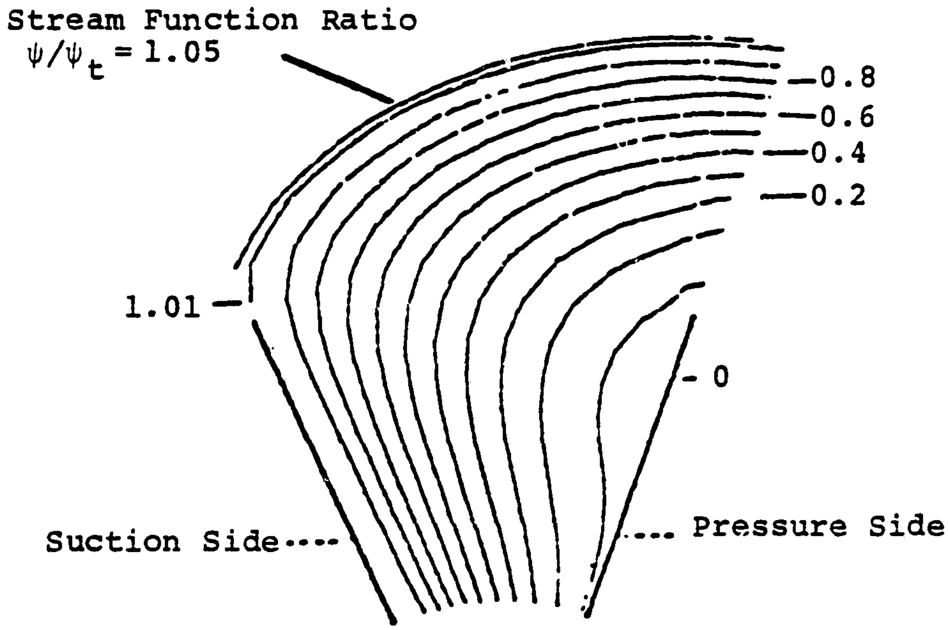

PREDICTED CASE 2

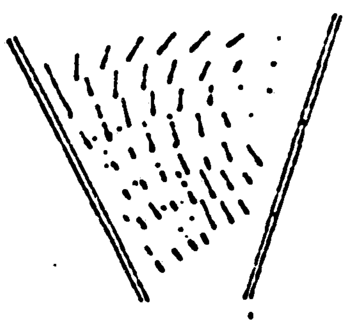

EXPERIMENTAL CASE

FIG. 1.2. RELATIVE STREAMLINES FOR FLOW THROUGH MIXED FLOW TURBINE.

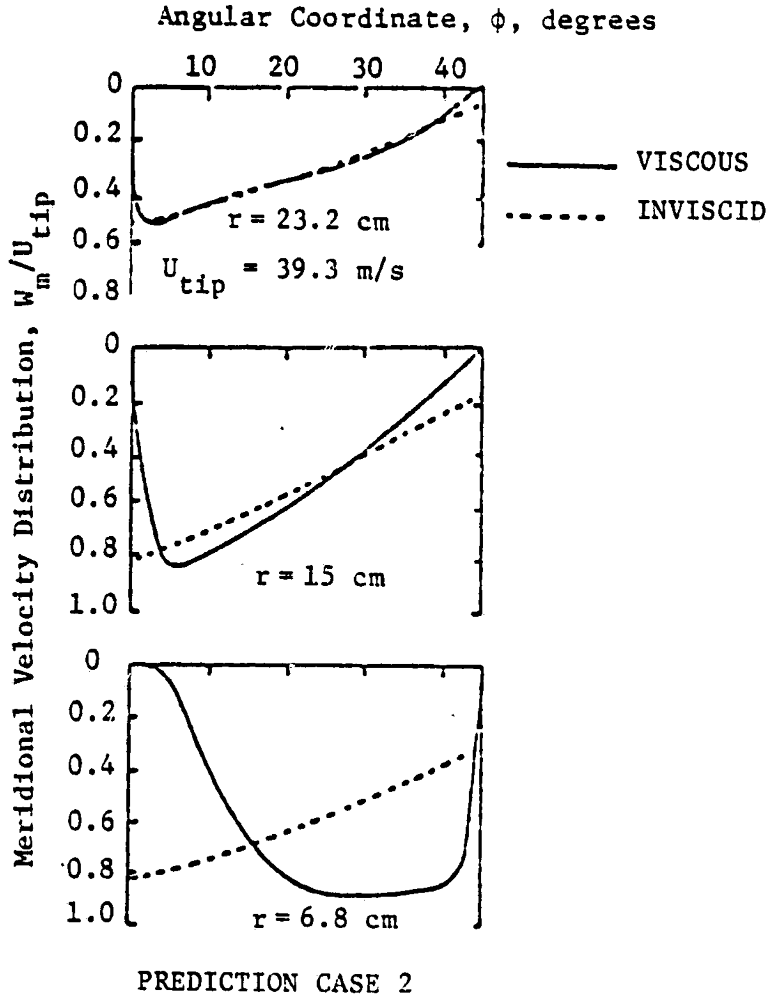

FIG. 1.3. NONDIMENSIONAL VELOCITY DISTRIBUTION AT DIFFERENT RADIAL LOCATIONS.

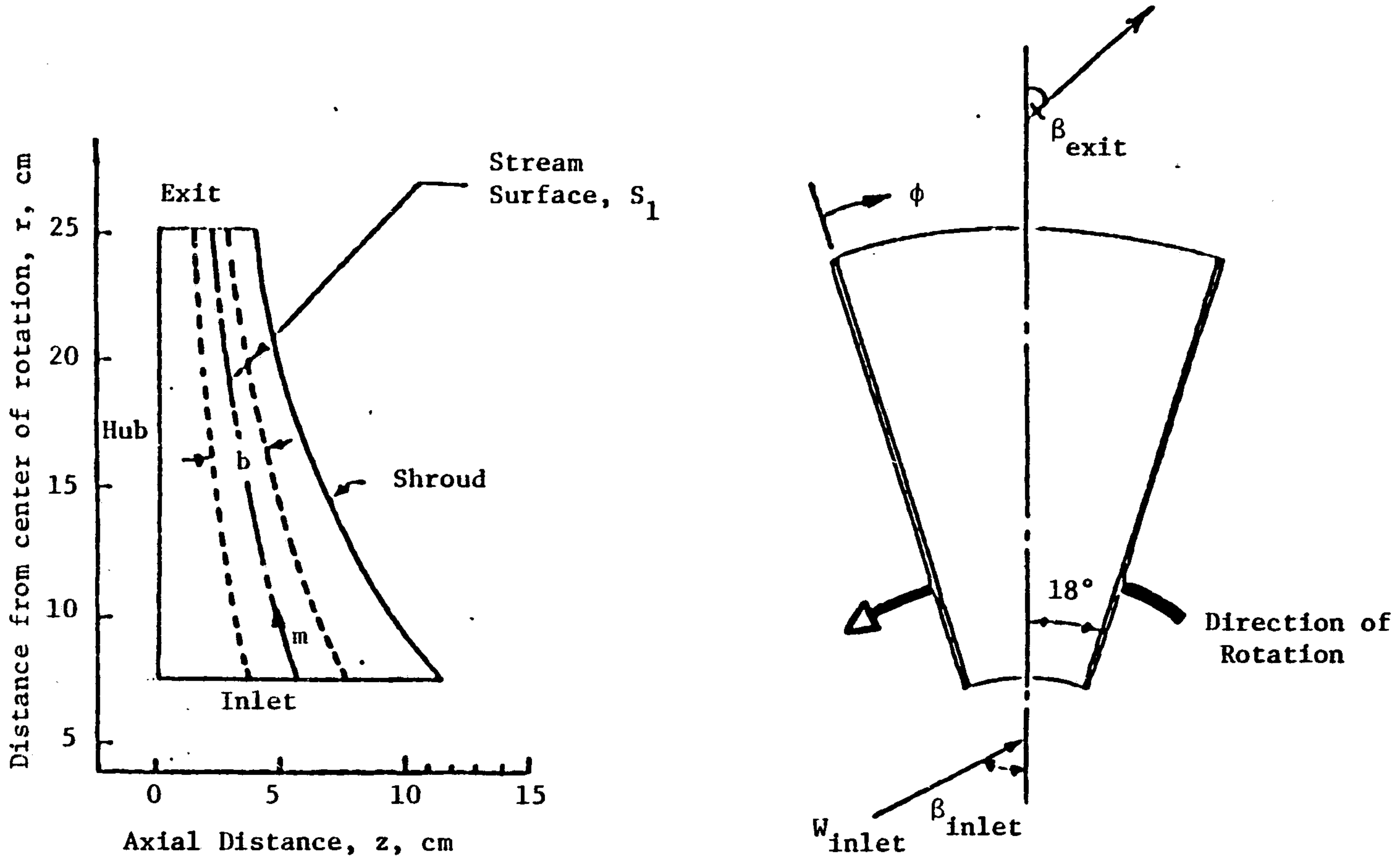

(a) MERIDIONAL VIEW

(b) BLADE-TO-BLADE VIEW

FIG. 1.4. HUB-SHROUD PROFILE WITH THE STREAM SURFACE, S_1, USED FOR BLADE-TO-BLADE ANALYSIS (COMPRESSOR CASE).

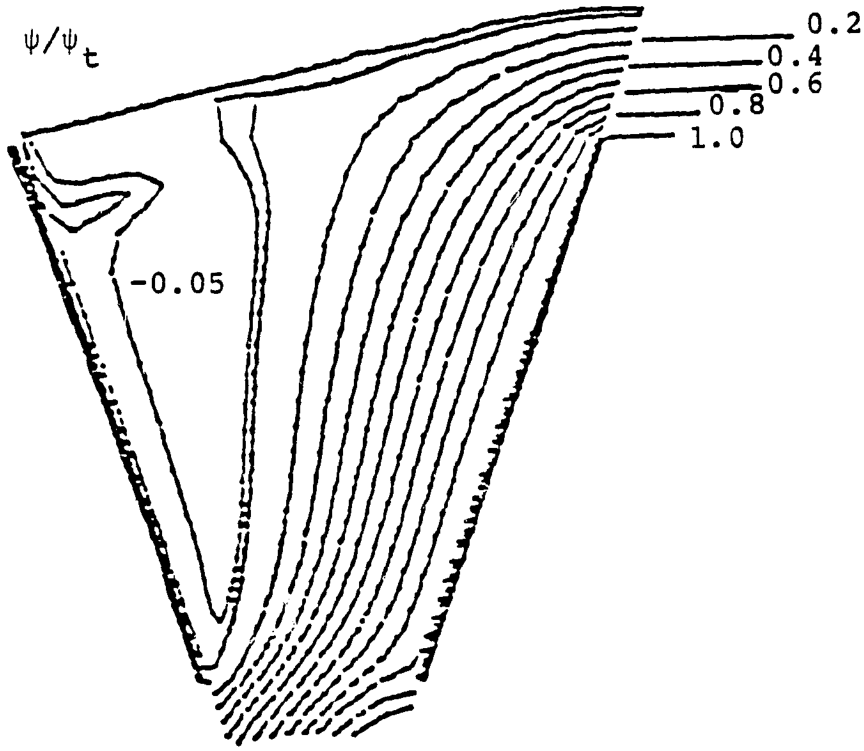

PREDICTED

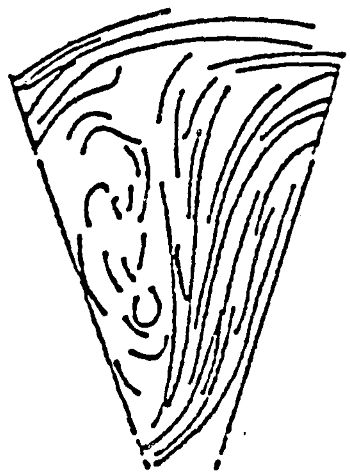

EXPERIMENTAL

FIG. 1.5. RELATIVE STREAMLINES FOR FLOW THROUGH RADIAL COMPRESSOR.

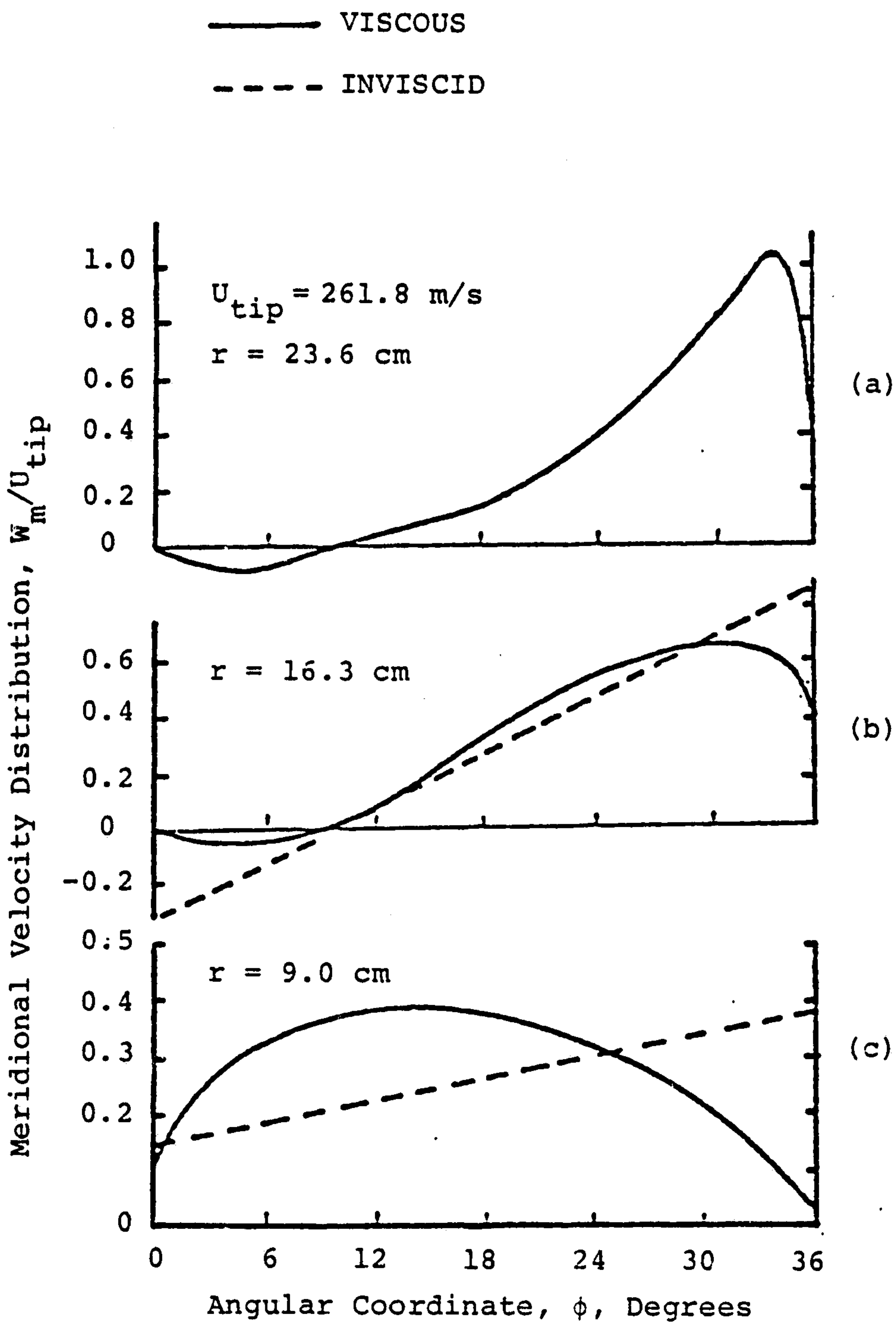

FIG. 1.6. VELOCITY PROFILES ACROSS THE COMPRESSOR PASSAGES AT DIFFERENT RADIAL LOCATIONS

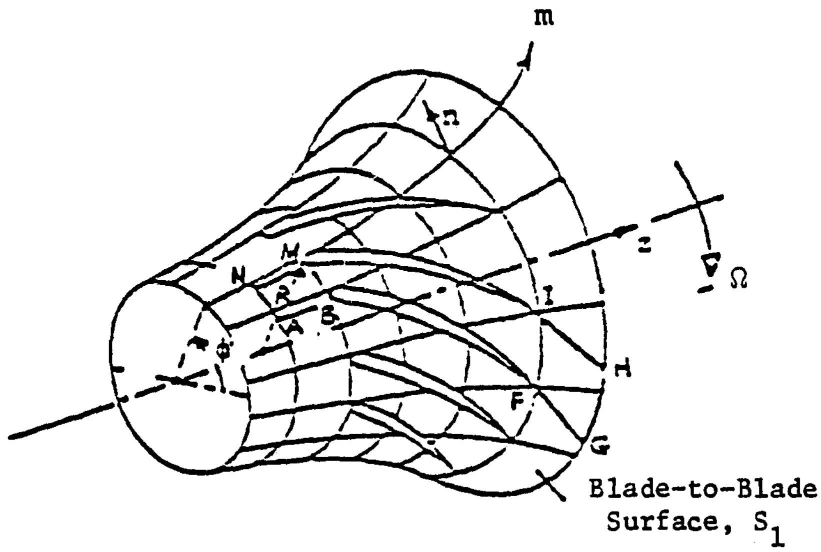

(a) BLADE ROW INTERSECTION WITH A STREAM SURFACE.

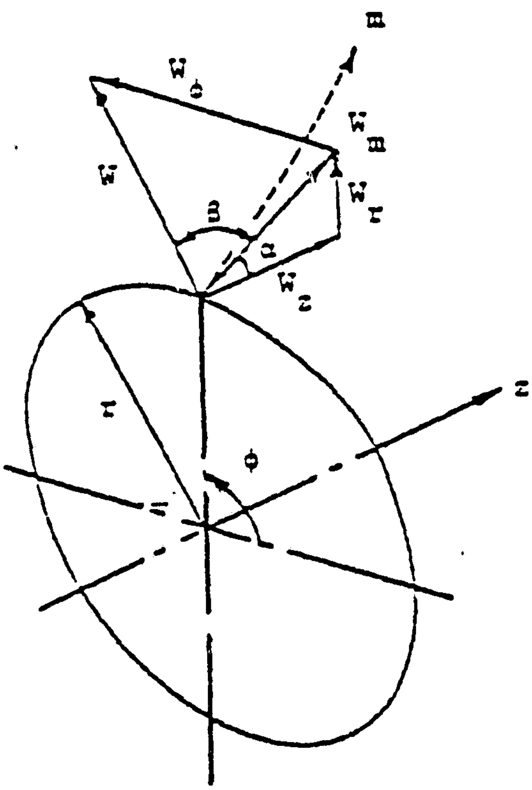

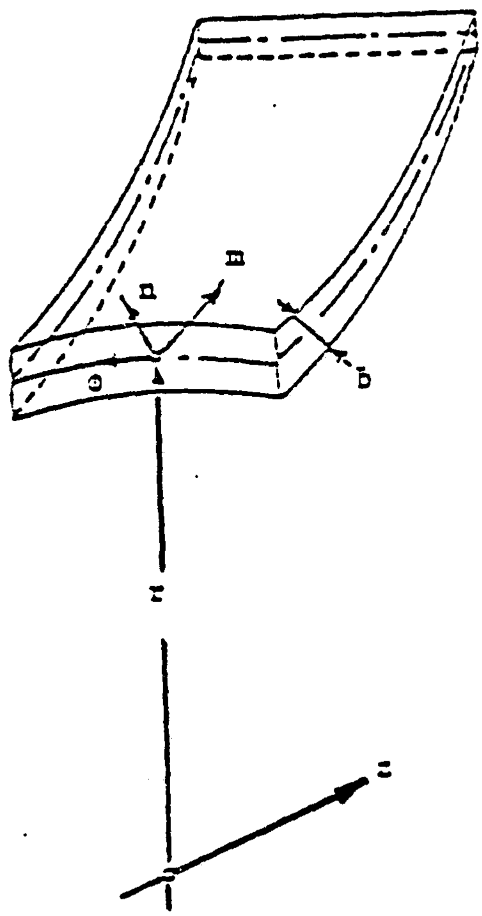

(b) COORDINATE SYSTEM AND VELOCITY COMPONENTS.

(c) DETAILS OF STREAM SURFACE COORDINATE SYSTEM WITH FINITE THICKNESS SHEET.

FIG. 1.7. BLADE-TO-BLADE STREAM SURFACE S_1.

1 5	6 10	11 15	16 20	21 25	26 30	31 35	36 40	41 50	51 60	61 70	71 80
AMU		PRDNO		TIP		TBLADE		RHOIP	WTFL	OMEGA	
BTI		BTO		BLADE		BIN		RTIP	RIN		
MXBI	MXBO	MX	NBBI	ITRB	IPRINT						

1 14	15 28	29 42	43 56	57 79	
AMM(I)	R(I)	SAL(I)	BRO(I)		
UTR(I,N)	VIR(I,N)	VIC(I,N)	UIC(I,N)	THETA(I,N)	

FIG. 1.8. INPUT FORM

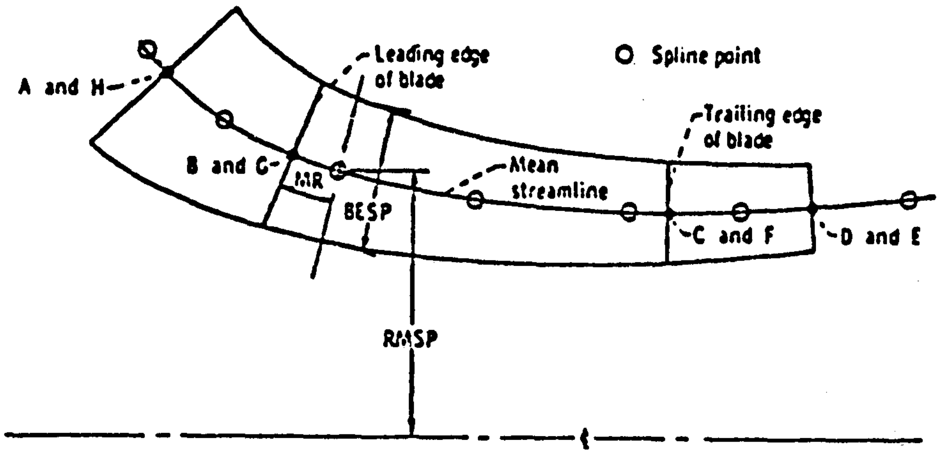

(a) MERIDIONAL PLANE

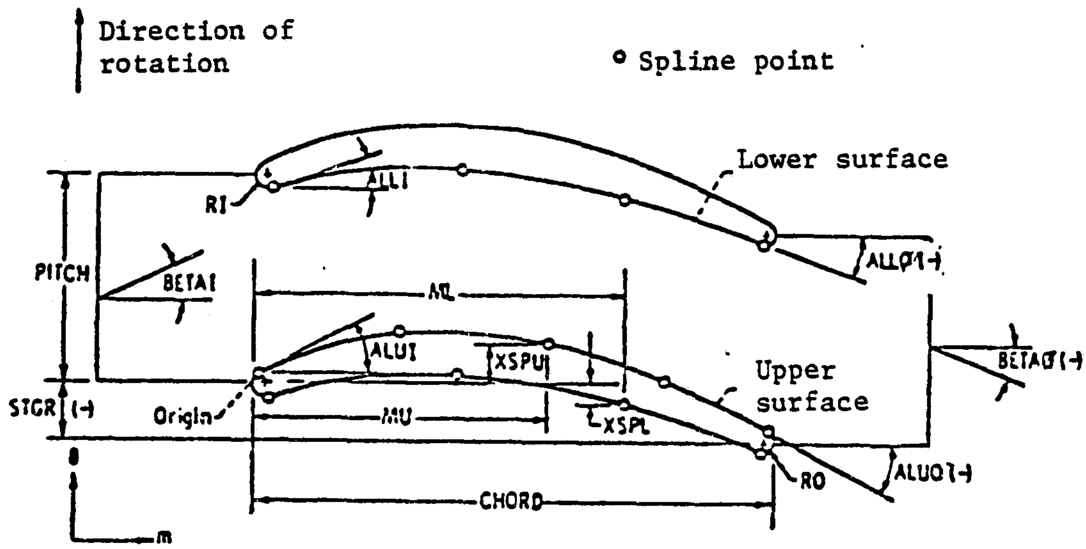

(b) BLADE-TO-BLADE COORDINATES ON STREAM SURFACE.

FIG. 1.9. GEOMETRIC VARIABLES REQUIRED AS INPUT.

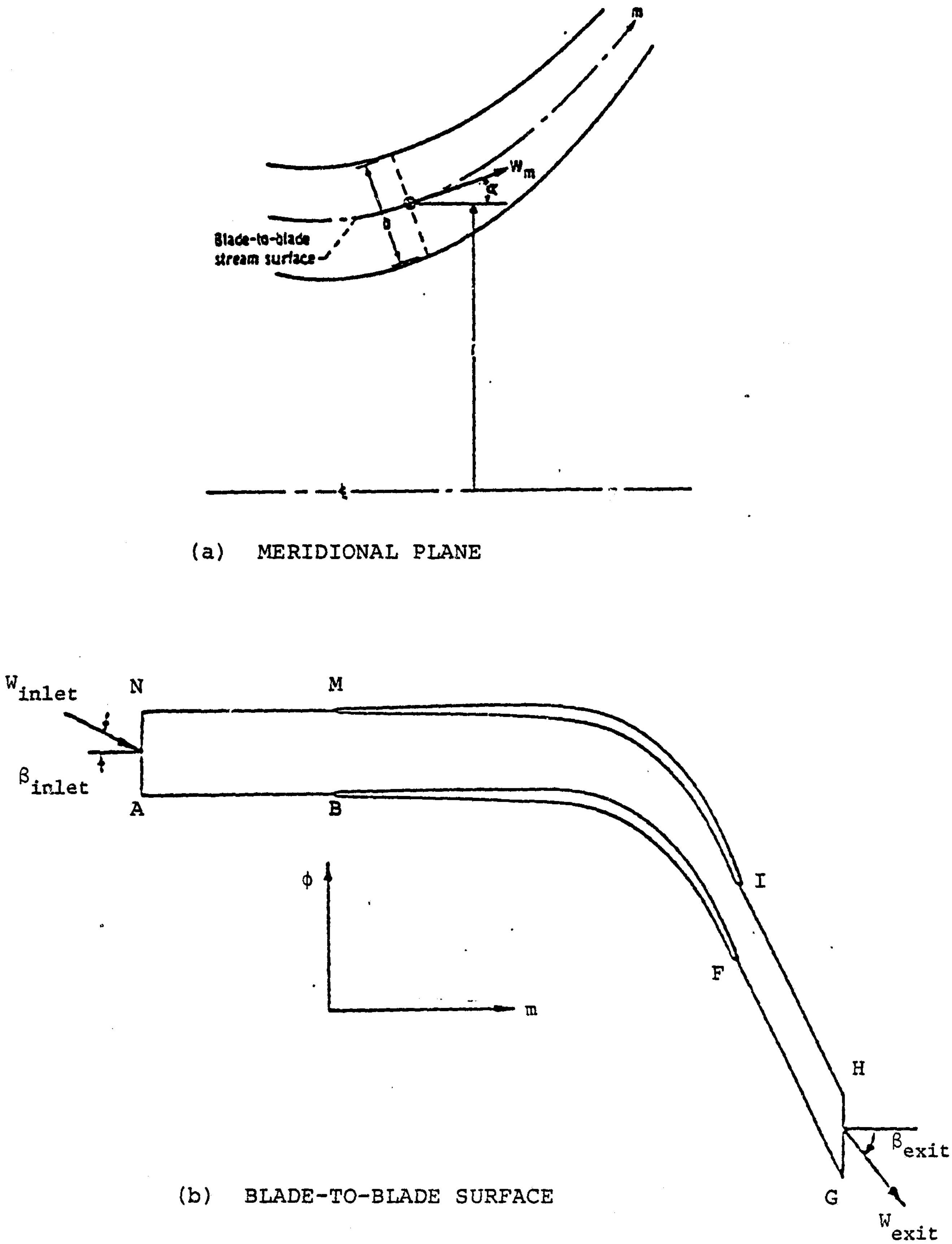

FIG. 1.10. COMPUTATIONAL DOMAIN IN THE PHYSICAL SPACE.

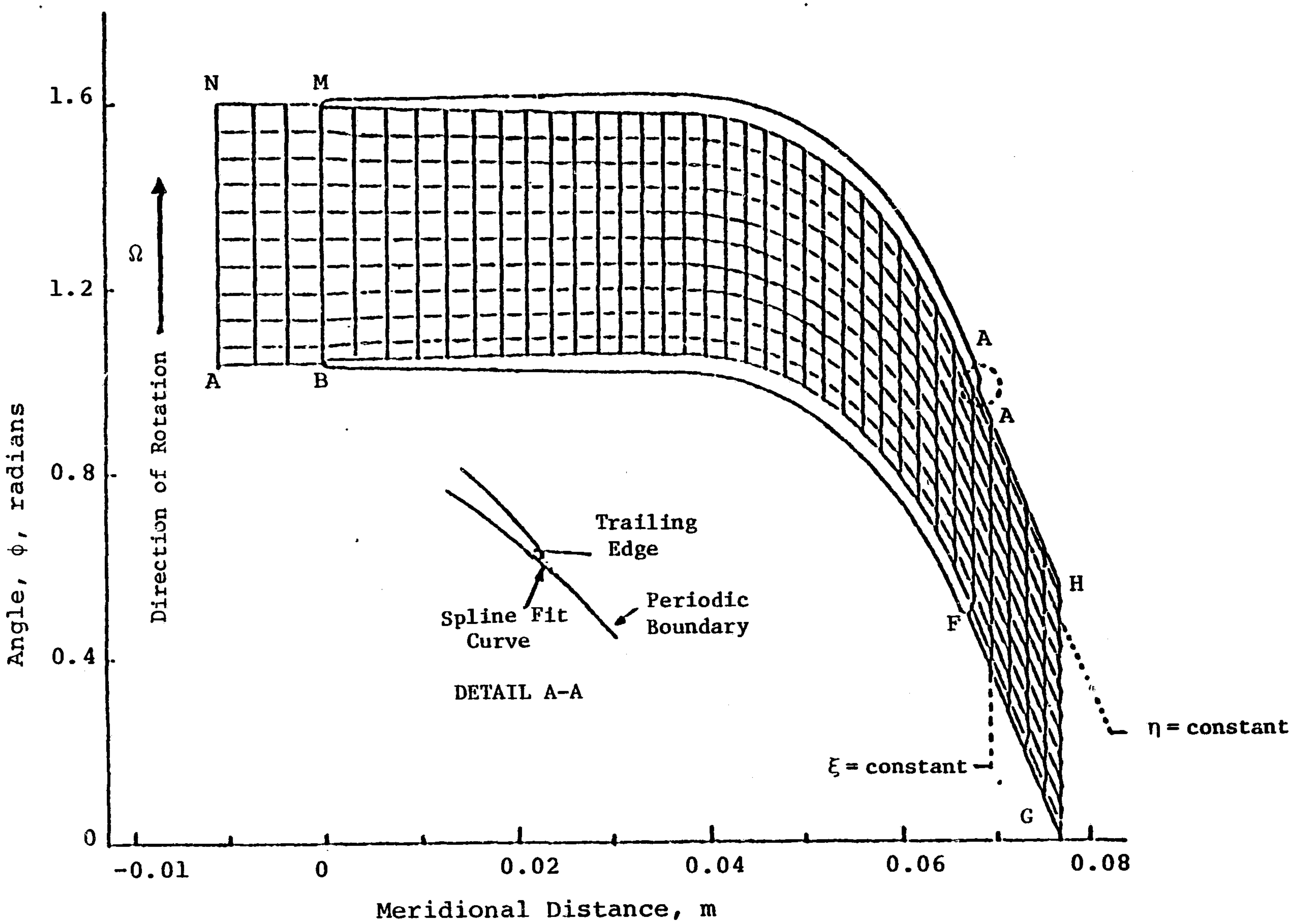

FIG. 1.11. TYPICAL MESH IN BLADE-TO-BLADE SOLUTION REGION.

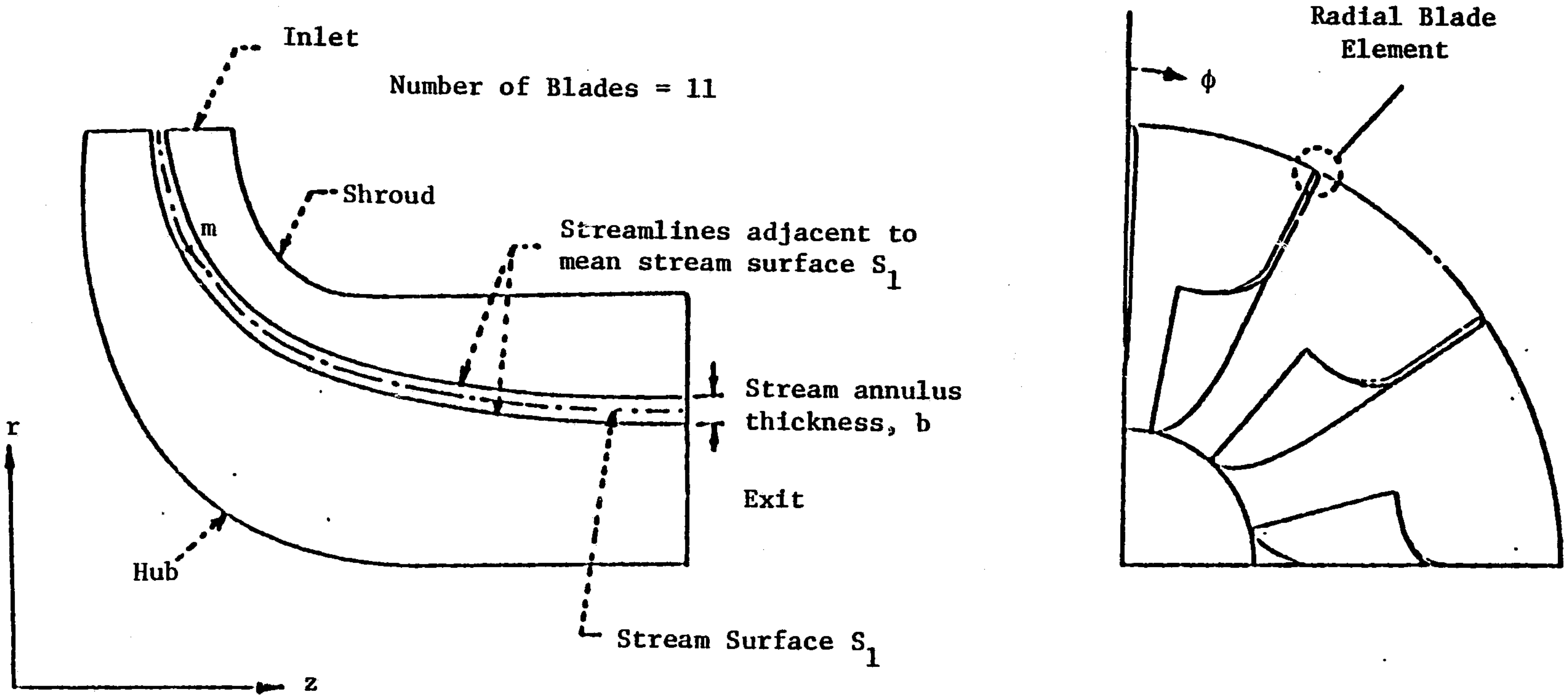

(a) MERIDIONAL VIEW

(b) BLADE-TO-BLADE VIEW (SCHEMATIC)

FIG. 2.1. HUB-SHROUD PROFILE WITH STREAM SURFACE S_1, USED FOR BLADE-TO-BLADE ANALYSIS.

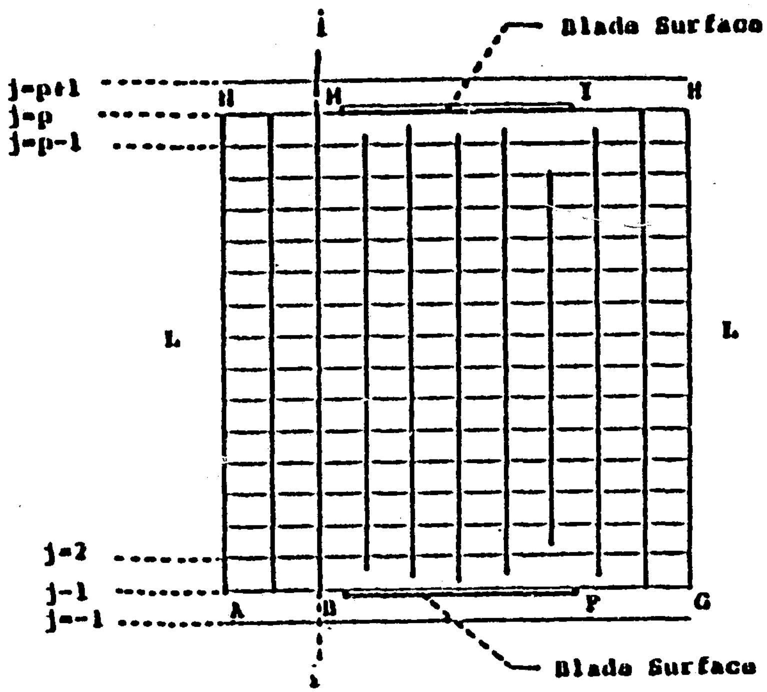

(a) GRID ROW ORDERING

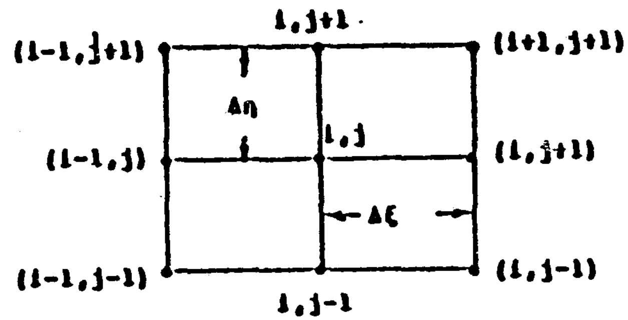

(b) GRID STRUCTURE FOR INTERIOR POINTS

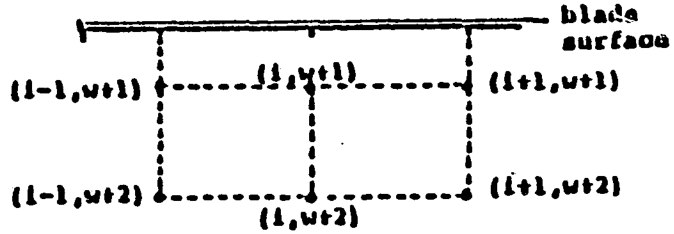

(c) POINTS NEAR A BLADE BOUNDARY

FIG. 2.2. GRID ORDERING SYSTEM IN THE TRANSFORMED DOMAIN

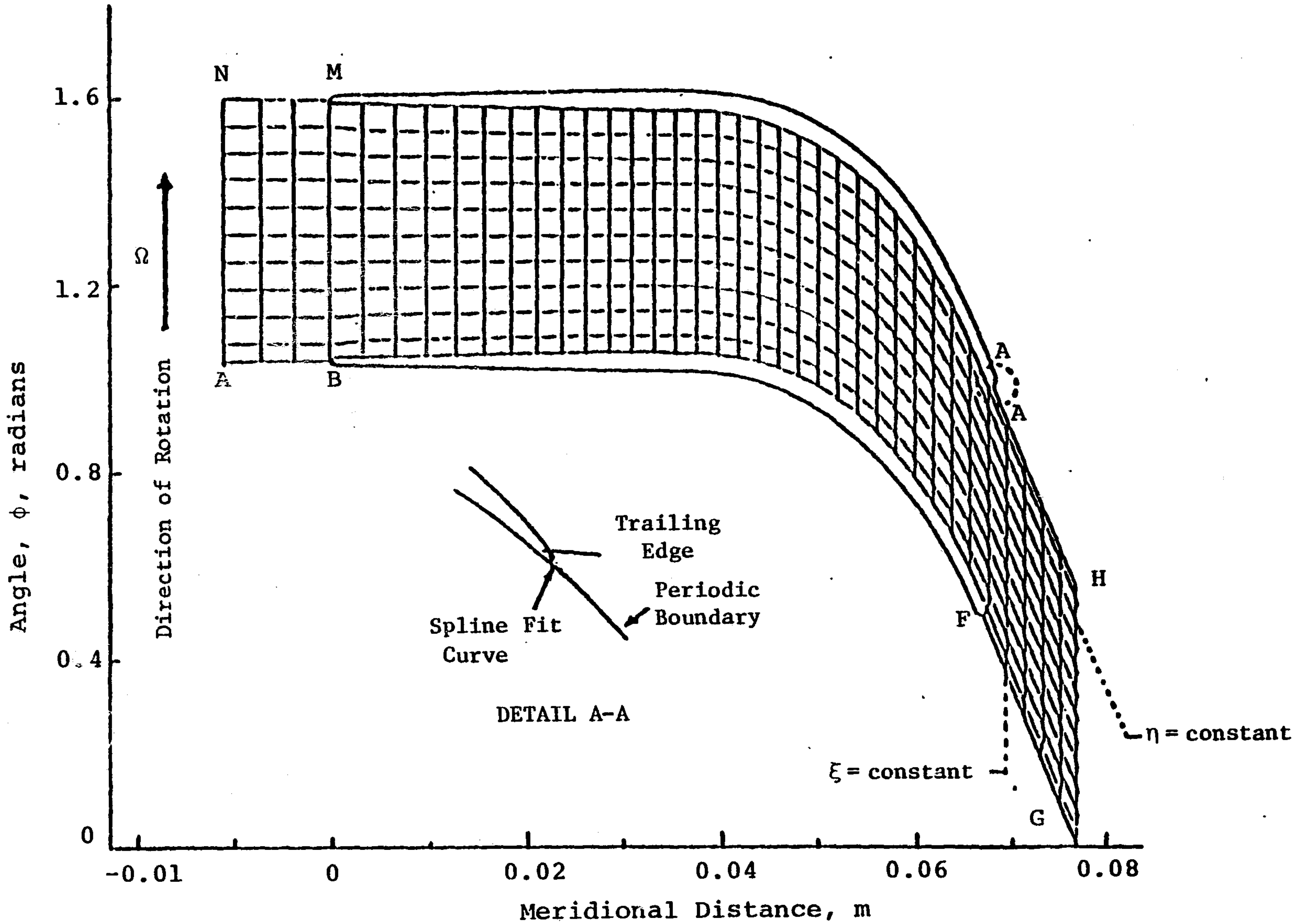

FIG. 2.3. BOUNDARY FITTED COORDINATE SYSTEM FOR THE MIXED FLOW TURBINE ROTOR.

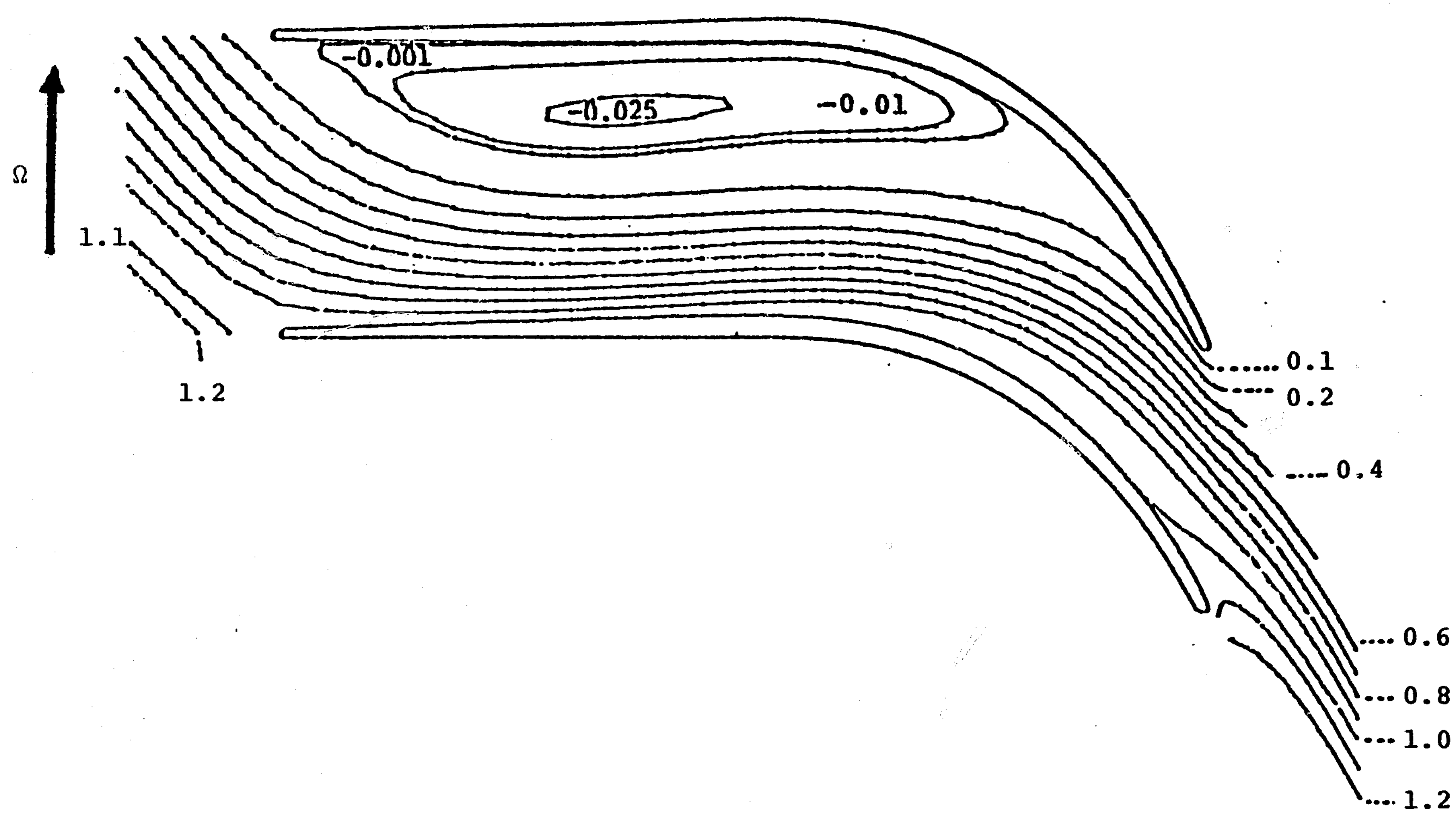

FIG. 2.4. RELATIVE STREAMLINES FOR FLOW THROUGH MIXED FLOW TURBINE.

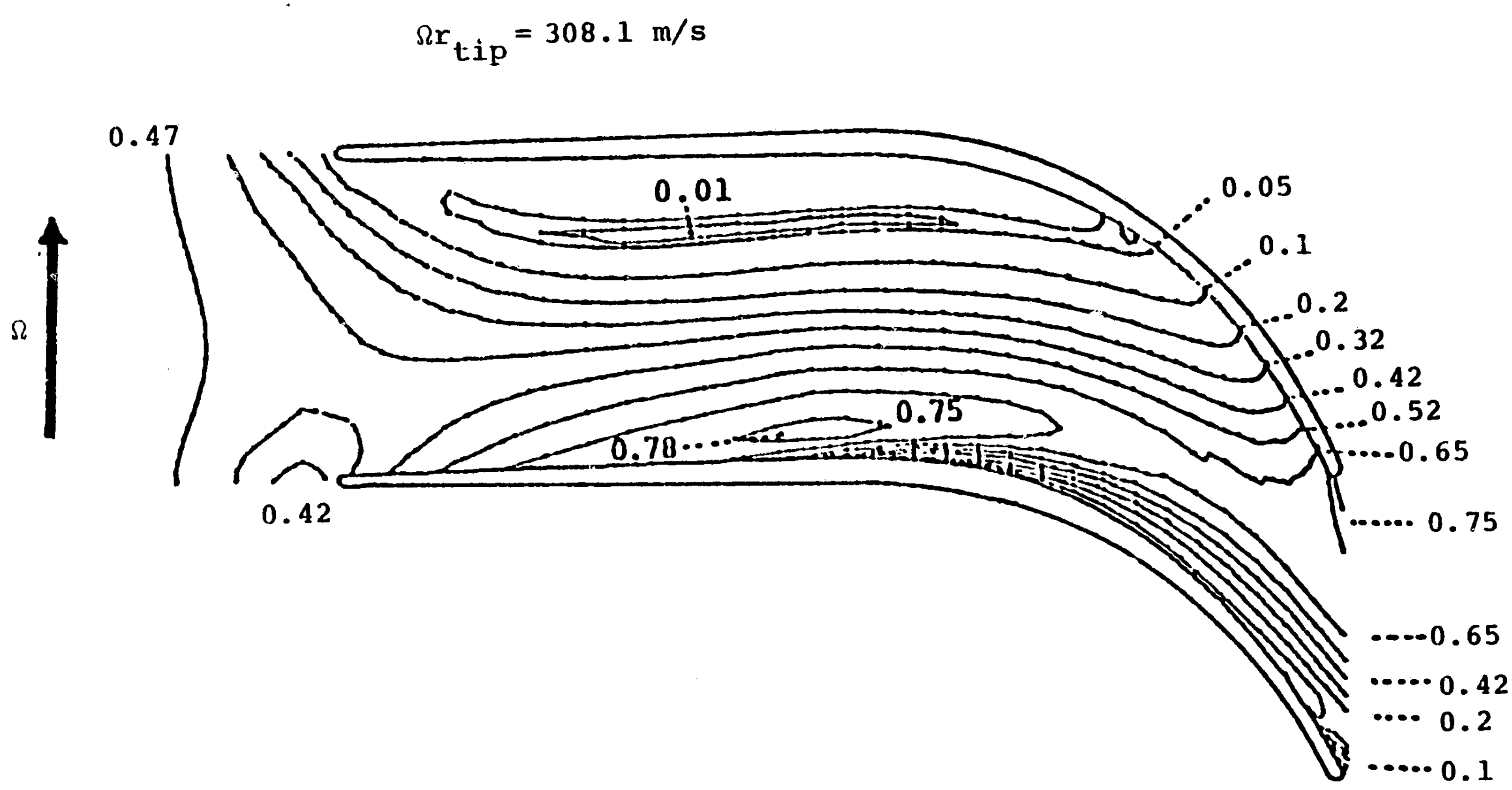

FIG. 2.5. RELATIVE VELOCITY DISTRIBUTION $(W/\Omega r_{tip})$

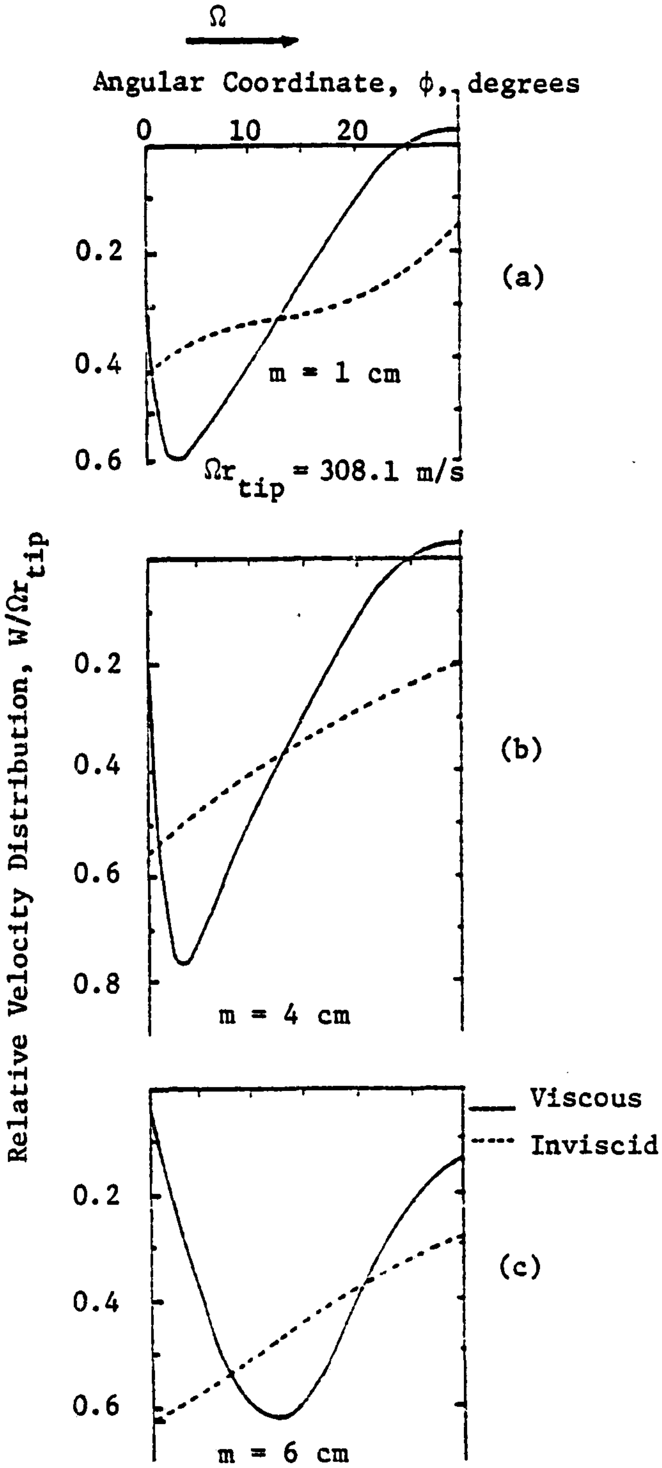

FIG. 2.6. NONDIMENSIONAL VELOCITY DISTRIBUTION AT DIFFERENT MERIDIONAL LOCATIONS.

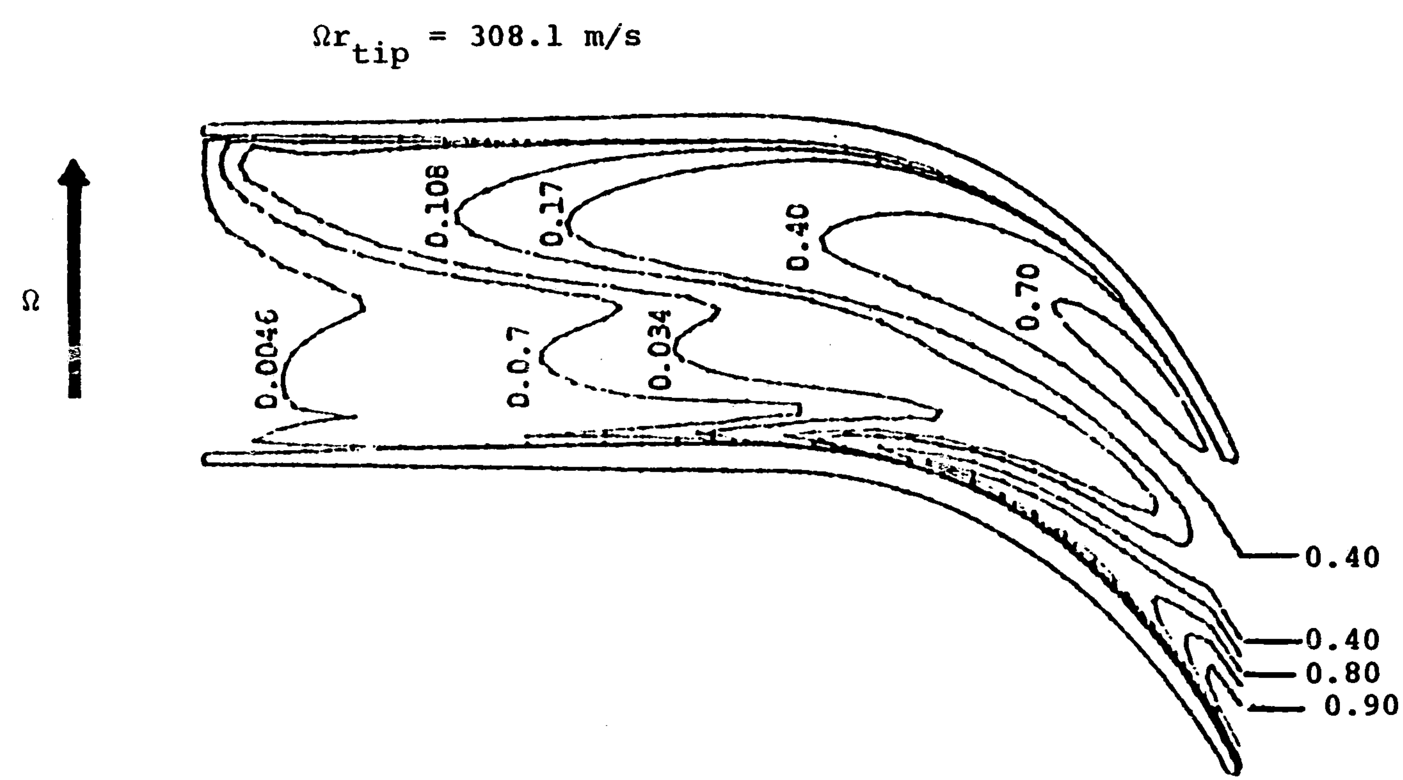

FIG. 2.7. KINETIC ENERGY OF TURBULENCE DISTRIBUTION $[(E/\Omega^2 r_{tip}^2) \times 10^2]$

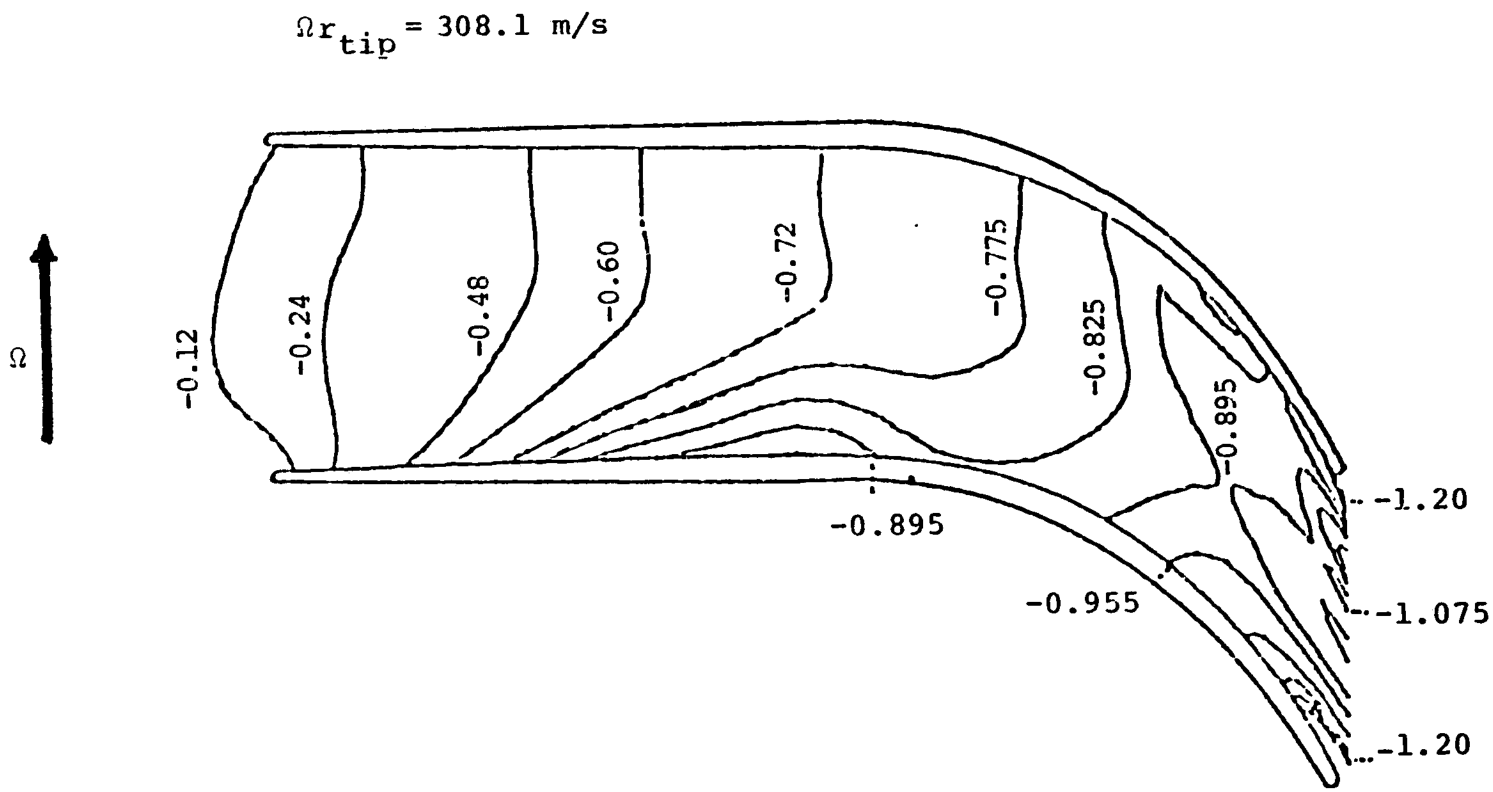

FIG. 2.8. STATIC PRESSURE DISTRIBUTION $[(p-p_{inlet})/\frac{\rho}{2g}\,\Omega^2 r_{tip}^2]$

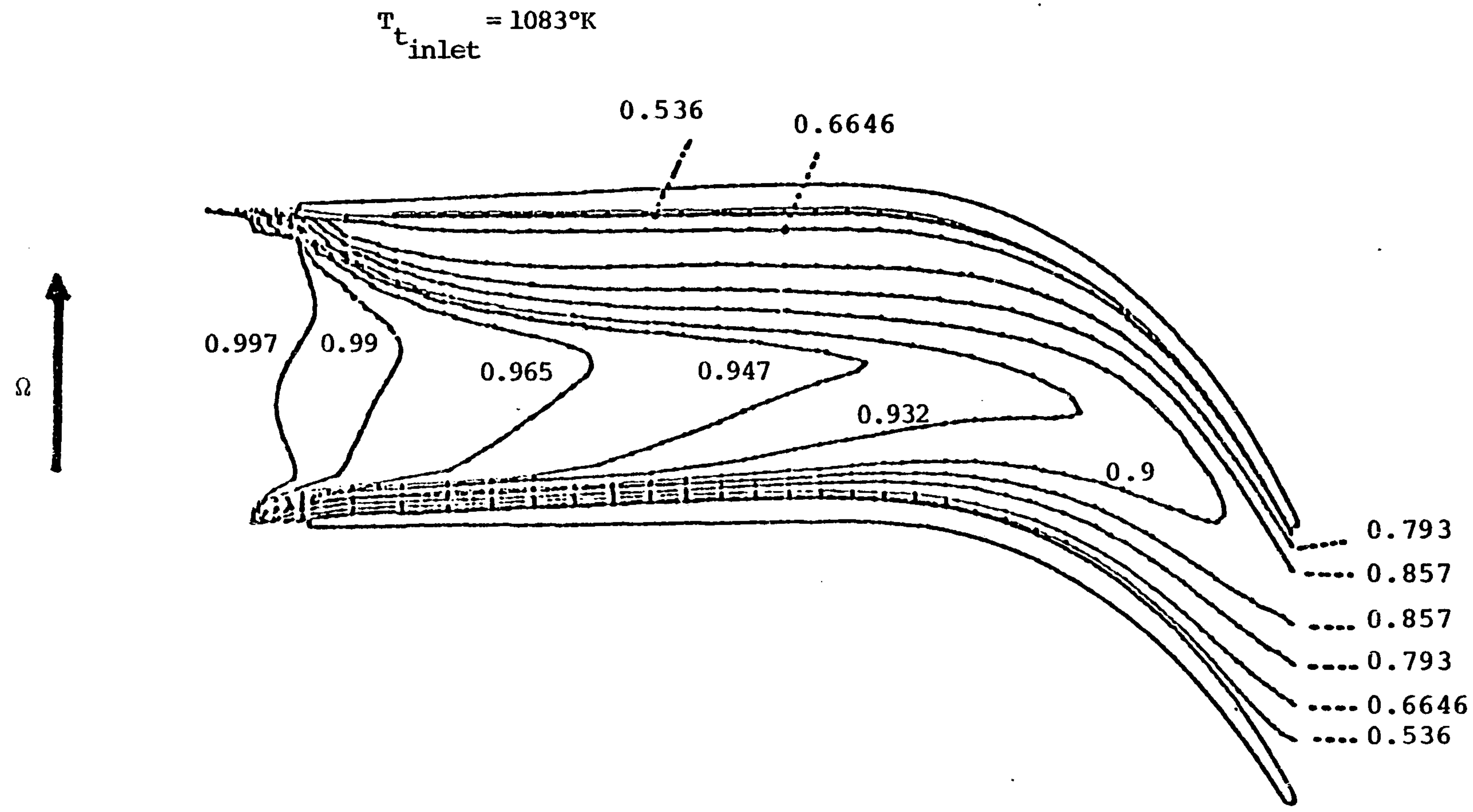

FIG. 2.9. STATIC TEMPERATURE DISTRIBUTION $[T/T_{t_{inlet}}]$